Advancing a Molecular Theory of Disease

The Highlights Lecture is presented at the closing session of each SNM Annual Meeting by Henry N. Wagner, Jr., MD. This year's lecture was presented on June 18 in New Orleans, LA. This was the 31st year in which Wagner delivered the lecture, and 2008 also marks the 40th anniversary of the publication of his seminal text, Principles of Nuclear Medicine. *Past SNM presidents Alexander McEwan, MD, and Peter Conti, MD, PhD, introduced the lecturer.*

As always, this meeting has been absolutely wonderful, in no small part because of the combined efforts of many of the organizers and participants. I would like to begin by thanking Virginia Pappas and the excellent staff of SNM. Credit also goes to Fred Fahey, DSc, chair of the Scientific Program Committee, and his team in selecting the presentations for this meeting and continuing to ensure that these are of such high quality. Thanks, too, to the officials and conscientious staff of the New Orleans Morial Convention Center for the tremendous amount of work it takes over many days to make the metaphorical trains run on time for an event such as this meeting.

Every year I pick a theme for this highlights talk, and this year I've chosen to spotlight the movement in which we are all participating in advancing a molecular theory of disease. Theories of disease, of course, have been around since before recorded history. In relatively modern times, the cell theory of disease was first proposed in 1858 by Rudolph Virchow (1821–1902). The germ theory of disease was proposed in 1862 by Louis Pasteur (1822–1895). These theories and their subsequent validation in scientific research provided new ways of organizing and understanding medical knowledge and applying that knowledge across an extraordinarily complex range of health challenges.

Molecular imaging simplifies the mind-boggling complexity of the human body. For example, the human body has 100 billion cells with 20,000 different molecular species per cell, each cell containing 100 million molecules. The human body contains 10^{11} neurons and 10^{15} synapses that have presynaptic neuronal vesicles, each vesicle of which contains 5,000 neurotransmitter molecules. I believe that many of you are to be congratulated for already working productively under the general framework of a new theory that I think will equal those of Virchow and Pasteur by creating the platform for future medicine. This is the "molecular theory" of disease. Derived from molecular imaging, this theory will provide the infrastructure for a revolutionary advance in scientific medicine. When we look at the billions and billions of molecules in the human body, we can feel secure that this is a field that will remain vital and productive for centuries.

Henry N. Wagner, Jr., MD

The essence of life is the recognition of molecules by molecules. Much of modern nuclear medicine has to do with labeling molecules that will be targeted at specific molecules or parts of molecules in the body, for imaging or therapy and sometimes for both. One example of molecular labeling was in the presentation at this meeting by Knešaurek and colleagues from the Mt. Sinai Medical School (New York, NY) on the use of ^{111}In-white blood cell SPECT/CT and MR imaging in tracking radiolabeled molecules to assess appropriate surgical approaches in the diabetic foot. The authors found that the CT study in ^{111}In SPECT/CT can be used to accurately fuse and compare SPECT and MR images in these patients. Figure 1 shows a fused image in a 24-y-old woman with an infected foot. The image shows osteomyelitis and soft tissue disease and provided valuable information that affected surgery and management. I selected this as the SPECT/MR Image of the Year for 2008.

Moving from the cellular into the molecular domain, we can look at a presentation from Castelluci and colleagues from the Azienda Ospitaliero Universitaria di Bologna (Italy) on the use of ^{68}Ga-DOTA-NOC PET to evaluate unusual neuroendocrine tumors. Figure 2 is a 3D PET/CT image in a 33-y-old man who had been referred for restaging of a somatostatin receptor–expressing tumor in the left middle ear. This precise imaging technique revealed that the tumor was not confined to the ear and that the pituitary gland and lymph node were also involved. This knowledge helped his physicians amend and enhance treatment approaches. I selected this as the PET/CT Image of the Year for 2008. Together, these images illuminate both the anatomical and functional range of molecular imaging "from head to toe." These images represent the state of the art and clearly indicate that both PET and SPECT are here to stay.

PET, SPECT, and Beyond in Molecular Imaging

The 4 pillars of molecular imaging at the present time are PET, SPECT, CT, and MR imaging, with a fifth pillar, optical imaging, now making substantial inroads. Figure 3

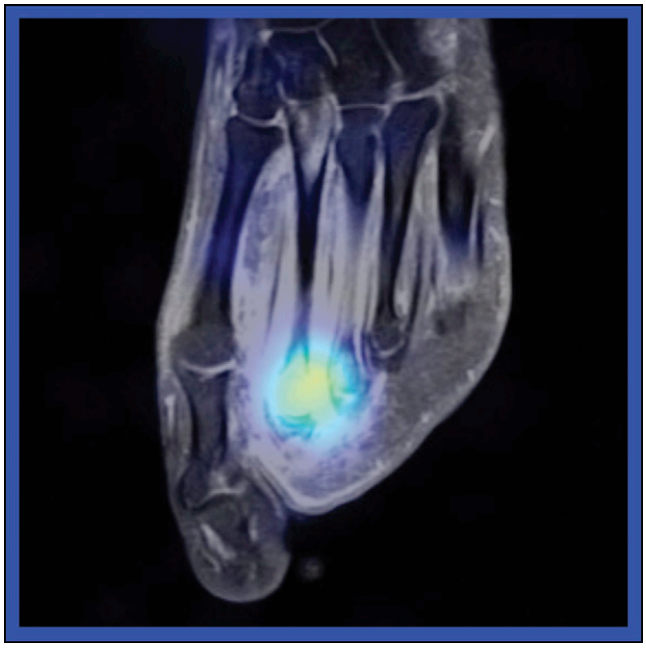

FIGURE 1. SPECT/MR Image of the Year. ^{111}In-white blood cell SPECT and MR imaging revealed osteomyelitis and soft tissue disease in this 24-y-old woman.

shows the growth in numbers of abstracts for presentations on PET (including PET/CT) and SPECT (including SPECT/CT) at the SNM Annual Meeting from 1982 to the present. Looking at the percentages of the total

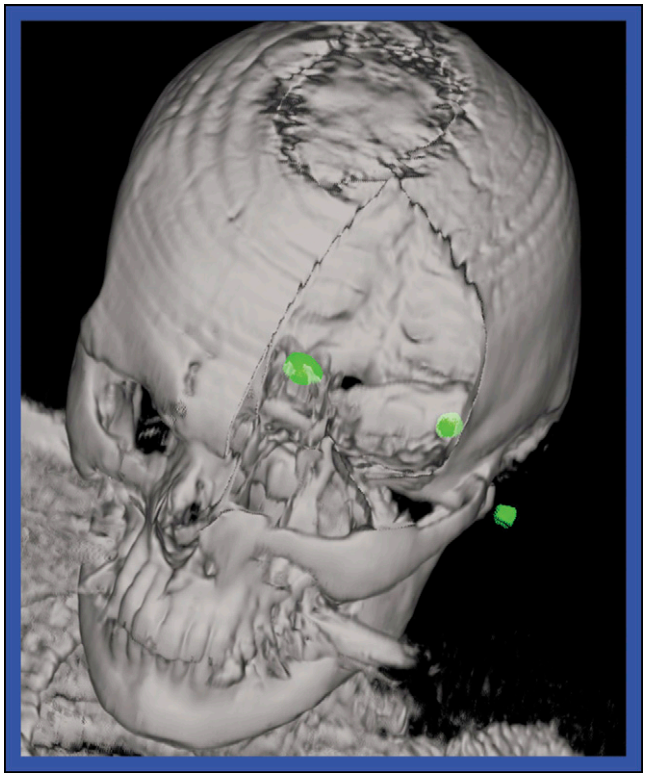

FIGURE 2. PET/CT Image of the Year. Molecular imaging of a somatostatin receptor–expressing tumor in a 33-y-old man showed additional involvement outside the ear.

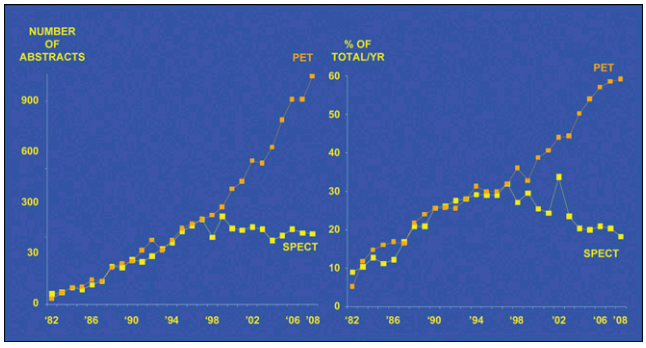

FIGURE 3. Left, number of PET and SPECT presentations at SNM annual meetings, 1982–2008. Right, PET and SPECT presentations as percentages of total presentation at each meeting, 1982–2008.

presentations also shown in this figure, it is clear that PET still dominates. Although SPECT is declining slightly as a percentage of papers, it has plateaued at a high level in absolute numbers.

SPECT is alive and well and being used to explore new areas. Wiseman and colleagues from the Mayo Clinic (Rochester, MN), GE Healthcare (Princeton, NJ), the National Institute of Child Health and Human Development (Bethesda, MD), the University of Iowa (Iowa City), the Cleveland Clinic Foundation (OH), Cedars–Sinai Medical Center (Los Angeles, CA), and the University of Washington (Seattle) reported on the results of a multicenter trial of ^{123}I-metaiodobenzylguanidine (^{123}I-MIBG) scintigraphy in patients with known or suspected pheochromocytoma. The studies were performed in 150 patients, with resulting sensitivity and specificity for scintigraphy of 85% and 78%, respectively. These results confirmed the clinical utility of this approach in managing pheochromocytoma.

Serafini and colleagues from the University of Miami Hospital (FL), GE Healthcare (Princeton, NJ), Mt. Sinai Hospital (New York, NY), and Piedmont Hospital (Atlanta, GA) reported on a study assessing the impact of SPECT on the interpretation of ^{123}I-MIBG studies in the evaluation of 200 children and adults with known or suspected pheochromocytoma or neuroblastoma. They found that ^{123}I-MIBG scintigraphy had a sensitivity and specificity of 81% and 79%, respectively. The researchers noted that although this technique provided a small improvement in quantitative performance, the use of SPECT assisted the readers' interpretation in almost half of patients studied.

Haug and colleagues from the Ludwig-Maximilians University (Munich, Germany) compared the diagnostic value of ^{68}Ga-DOTA-TATE, a positron-emitting tracer that binds to somatastatin receptors, with that of ^{18}F-DOPA PET/CT in patients with histologically proven neuroendocrine tumors. In general diagnosis was better with the gallium tracer, with half of ^{18}F-DOPA studies as false-negatives. However, uptake of ^{18}F-DOPA, because it is a precursor of monoamine, was correlated with increased serum levels of serotonin. The authors concluded that ^{68}Ga-

DOTA-TATE PET should be considered as a first-line imaging modality for well-differentiated neuroendocrine tumors, whereas ^{18}F-DOPA might be useful only in serotonin-positive cases with negative ^{68}Ga-DOTA-TATE PET.

As is the case with many agents, therapy follows diagnosis. Cwikla and colleagues from the Medical Center of Postgraduate Education and the Hospital Ministry of Internal Affairs and Administration (Warsaw, Poland), the OBRI-Polatom Radioisotope Center (Otwock-Swierk, Poland), and the Royal Free Hospital (London, UK) reported on the benefits of ^{90}Y-DOTA-TATE somatastatin-binding therapy in patients with progressive metastatic neuroendocrine tumors. The study included 56 patients (26 women, 30 men; mean age, 52 y; range, 23–72 y) with histologically proven, extensive, nonresectable, and progressive neuroendocrine carcinomas. The patients underwent a total of 168 treatments. Therapy was found to be effective, with standard doses carrying a low risk of myelotoxicity. Figure 4 shows an example image of a patient at baseline (before treatment) and at 12 m after initiation of treatment.

Important advances are being made in generators. New ^{90}Sr/^{90}Y generators for radiotherapeutic applications, developed with funding by the International Atomic Energy Agency (IAEA) in association with investigators in India, were described by Chakravarty and colleagues from the Bhabha Atomic Research Centre in Mumbai and from the IAEA. These generators can produce up to 100 mCi (3.7 GBq) levels. Radiochemical separation is effective, and radionuclidic purity is >99.998%, suitable for direct labeling of biomolecules. These generators are simple to operate and can be scaled up and automated. This type of collaborative and beneficial work is an example of what the IAEA continues to do for the field of nuclear medicine, particularly in developing countries.

Scott and Australian colleagues from Austin Hospital, Peter MacCallum Cancer Centre, and the Australian and New Zealand Association of Physicians in Nuclear Medicine (Melbourne); Wesley Hospital (Brisbane); Royal Adelaide Hospital; Liverpool Hospital (Sydney); and the Sir Charles Gardner Hospital (Perth) compared the effects of ^{18}F-FDG PET and ^{68}Ga scanning in disease staging and management of patients with low-grade non-Hodgkin's lymphoma. The study included 74 patients, all of whom underwent PET scanning and 16 of whom underwent gallium scanning. Gallium detected additional lesions in 6 of the 16 patients (38%), but ^{18}F-FDG detected additional lesions in 10 of the 16 patients (63%). Patients with additional lesions detected by PET had a significantly inferior disease-free survival and a lower complete response. Patient treatment was changed in 7 of the 16 patients (44%) based on ^{18}F-FDG PET criteria and in only 3 of the 16 patients (19%) based on gallium scanning results. A big difference, however, is that ^{68}Ga is available from a generator, making it an option for those who do not have cyclotrons or a supply of ^{18}F-FDG.

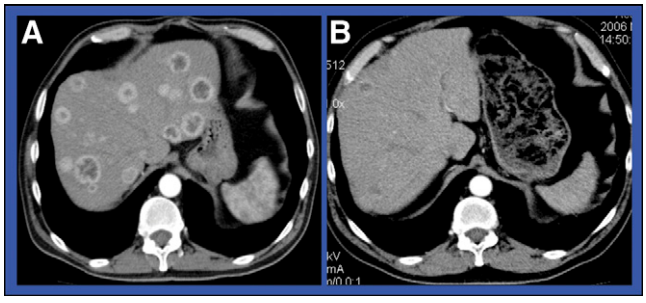

FIGURE 4. Example images at baseline (A) and at 12 mo (B) after initiation of ^{90}Y-DOTA-TATE somatastatin-binding therapy in a patient with a progressive metastatic neuroendocrine tumor.

The utility of molecular-based imaging in screening of asymptomatic individuals is a topic of growing interest annually at this meeting. Minamimoto and Japanese colleagues from Yokohama City University, the Institute of Biomedical Research and Innovation (Kobe), the Nishidai Clinic Diagnostic Imaging Center (Tokyo), Atsuchi Memorial Clinic PET Center (Kahoshima), and Tohoku University (Sendai) reported on a nationwide survey of the performance of ^{18}F-FDG PET and PET/CT for cancer screening conducted in 2005 and 2006. Researchers at 97 centers completed surveys and responded with the results of imaging in 87,057 healthy individuals who had positive PET and/or combined screening tests. Of these, 992 (1.14%) were found to have previously undetected cancers. Among these were colon/rectum (218 cases), thyroid (194 cases), lung (173 cases), breast (64 cases), prostate (91 cases), and gastric (56 cases) cancers.

Isohashi and colleagues from the Osaka University Graduate School of Medicine (Suita, Japan) compared the accuracy of ^{18}F-FDG PET with that of CT or MR imaging in staging/restaging in patients with malignant lymphoma and in evaluating therapy response and recurrence. The study included 59 patients who had undergone chemo- or radiation therapy. Serial PET and CT/MR images were compared. PET and CT/MR imaging accuracies for staging/restaging were 92% and 84%, respectively. The corresponding figures were 84% and 50% for evaluation of treatment and 83% and 72% for screening of recurrence. In the 122 pathologic sites with discrepant findings between PET and CT/MR imaging, the accuracy of PET (76%) was significantly greater than that of CT/MR imaging for evaluation of treatment response.

In addition to monitoring response to drug therapy, we can also monitor the effects of surgical procedures. Zuo and colleagues from the Huashan Hospital and Ruijin Hospital (Shanghai, China) and the North Shore–Long Island Jewish Health System (Manhasset, NY) reported on modulation of metabolic brain function by bilateral subthalamic nucleus stimulation in the treatment of Parkinson's disease. Figure 5 shows the positioning of the intracranial electrodes for deep brain stimulation. Researchers found that bilateral subthalamic nuclear stimulation increased metabolism in the left midbrain and pons (Fig. 6) but decreased metabolism in

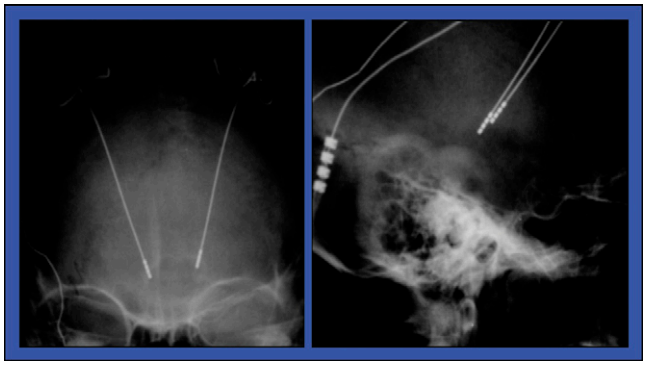

FIGURE 5. Positioning of intracranial electrodes for bilateral subthalamic nucleus stimulation in the treatment of Parkinson's disease.

the right lentiform nucleus and cerebellum, as well as in the bilateral thalamus and precuneus. Clinical symptoms showed some improvement, leading the authors to conclude that deep brain stimulation is more likely to function by regulating the entire neuronetwork than by exciting or inhibiting specific areas.

What is the relationship of blood tests to molecular imaging in screening? Kong and colleagues from Yeungnam University Hospital (Daegu, South Korea) compared the sensitivities of ^{18}F-FDG PET/CT and serum carcinoembryonic antigen (CEA) levels in detection of recurrent colorectal cancer after curative surgical resection. The study included 715 patients who underwent both PET/CT and CEA level analyses. A final diagnosis of recurrence was proven histologically or radiologically in 79 patients (52 men, 27 women; mean age 60.7 ± 11.8 y). PET/CT detected suspicious lesions in 78 patients. Five of these 78 patients were positive only on CT (lung nodules), with no tracer uptake. Forty of the 79 patients (51%) showed increased serum CEA (>10 ng/mL), meaning that CEA levels were normal in almost half of these patients in whom PET/CT detected disease.

Champion and colleagues from the Rene Huguenin Cancer Research Center (Saint-Cloud, France) reported on the value of ^{18}F-FDG PET/CT in patients in whom rising tumor markers lead to a suspicion of recurrent breast cancer. The study included 238 consecutive, asymptomatic patients who presented with rising tumor markers over a mean follow-up of 34 mo (range, 12–67 mo). The researchers found that PET/CT sensitivity, specificity, positive and negative predictive values, and accuracy in detecting recurrence were 94.5%, 85.5%, 97.4%, 72.5%, and 92.5%, respectively. They concluded that ^{18}F-FDG PET/CT should be considered as a "one-stop shop" procedure for breast cancer recurrence, particularly in the setting of rising tumor markers.

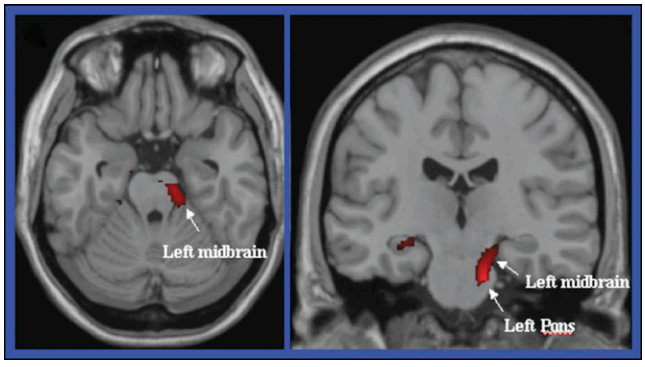

FIGURE 6. Bilateral subthalamic nucleus stimulation increased metabolism in the left midbrain and pons in individuals with Parkinson's disease.

How did ^{18}F-FDG become the tracer molecule of the 20th century? Are there lessons to be learned in looking at how FDG has attained this status? We can look at some of the successes and advantageous aspects of this tracer. First, FDG measures a key biochemical process (energy metabolism), and the results of FDG studies have been clearly linked to the enhancement of surgical decision making. Legislative support led to reimbursement by the Centers for Medicare and Medicaid Services (CMS) in the United States, in part as a result of early clinical adoption and promotion by industry. For some time, many regional suppliers have offered FDG, which is produced through easily automated chemical synthesis. ^{18}F has an appropriate and manageable half-life of 110 min. PET/CT images now appeal to radiologists and other physicians by relating visually familiar structure to function and biochemistry. The images we have to offer with ^{18}F-FDG PET/CT have gone from the old "unclear" nuclear studies to a more medically accessible clarity.

In my opinion, clinical radiotracer production in the future will be active at the national, regional, and institutional levels. The United States had 10 regional FDG distribution sites in 1996 and has 110 today. Japan has 10 FDG production sites, supplying 50 hospitals.

Hillner et al. reported in the May issue of the *Journal of Clinical Oncology* (2008;26:2155–2161) on initial results from the National Oncologic PET Registry (NOPR). NOPR collected questionnaire data from referring physicians on intended patient management before and after PET and PET/CT over a 1-y period. The results included 22,975 PET studies (83.7% of which were PET/CT) from 1,178 centers. Results showed that patient management changed in 37.2% of patients after PET or PET/CT. NOPR has now formally asked CMS to expand reimbursement for the use of ^{18}F-FDG PET for nearly all oncologic applications, with a response expected this fall.

I believe that personal acceptance of responsibility by the physician should be the primary regulatory mechanism of the future for imaging procedures—somewhat analogous to the responsibility that surgeons assume when they decide, with their patients, whether or not to proceed with specific types of surgery. The economist William H. Donaldson recently said, "There is a limit to how much regulation can do. In the final analysis, you could write all the rules you want, but there has to be a philosophy of ethical behavior that comes from human beings operating in a professional way."

Described at this meeting was a global imaging network that has been initiated and is already in use that will manage and archive every imaging study being considered in clinical use. Connected via the Hermes Solution, this network will provide secure remote access to users worldwide. This technology is already available. My proposal is that the U.S. Food and Drug Administration (FDA) approve a relatively small number of studies and make it possible for these studies to be carried out with a modified phase 4 approach; that is, all the studies must go into a central database. Such a database could have a server in the United States and one in Europe on which images could be recorded and continuously examined to make sure that the imaging procedures are safe and effective.

Shah and Srinivas from the Cleveland Clinic (OH) decribed an innovative reporting scheme for hybrid diagnostic examinations. Their approach in integrated reporting of both PET and diagnostic contrast-enhanced CT scans eliminates redundancy in performing separate modality-specific interpretations and provides a single cohesive answer to the clinical question. The elimination of discordant reports produces a clearer assessment of pertinent findings for the referring physician. Additional benefits include workflow efficiency and cost savings.

The Value of the Unexpected

Many studies presented at this meeting showed the importance of an expert observer in detecting and interpreting unexpected findings in PET and SPECT studies. I like the analogy of a modern airplane where a skilled pilot is still required, despite many automated features that enable the plane to "fly itself." Han and colleagues from Catholic University of Korea (Seoul, South Korea), for example, reported on the significance of incidental finding of focal uptake of ^{18}F-FDG in the prostate. Among 5,118 PET/CT images reviewed from a 4-y acquisition period, 62 cases showed incidental focal tracer uptake in the prostate. Of these, 52 had pathologic confirmation, clinical follow-up, radiologic images, or prostate serum antigen levels for inclusion in the final analysis. Among these 52 individuals, 2 patients (3.8%) were confirmed to have malignant lesions. The authors concluded that although focal ^{18}F-FDG uptake in the prostate was incidentally noted in 1.2% of PET/CT scans and that only a small percentage of these were malignant, "further evaluation is necessary when the focal uptake is seen discretely in the periphery."

Wu and colleagues from the Chi Mei Medical Centers (Liouying and YungKang, Taiwan) reported on incidental findings of tuberculosis in 2,850 patients undergoing ^{18}F-FDG PET/CT scanning for oncologic indications. Thirty-four patients were found to have tuberculosis in lesions that accumulated tracer in specific nodular patterns. Figure 7 shows an example scan from a 57-y-old man in whom regions of glucose accumulation had a diffuse appearance that was at first thought to be pneumonia but was described by these investigators as characteristic of tuberculosis. In the images acquired after 6 mo of tuberculosis treatment, these lesions had disappeared, although residual accumulation can be seen in the cancerous lung lesions.

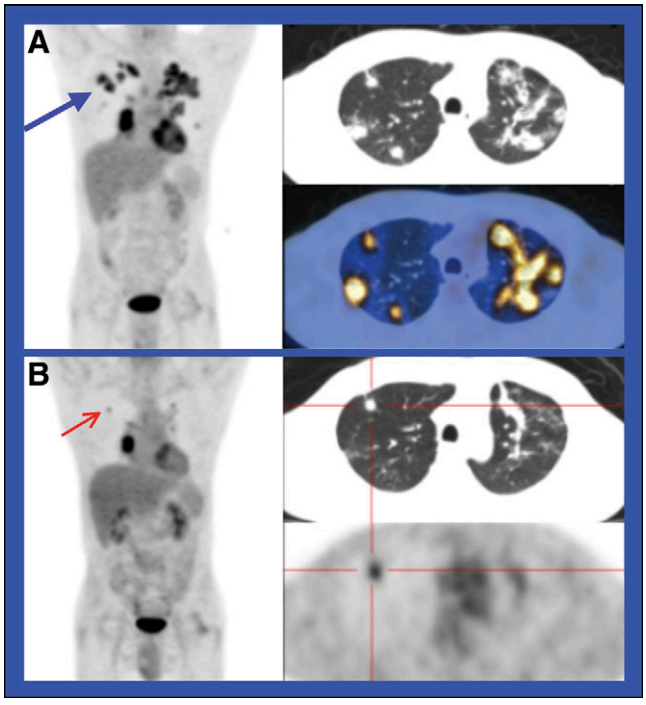

FIGURE 7. In this 57-y-old man with lung cancer, incidental findings of diffuse tracer uptake (A panel) suggested pneumonia but were found to be tuberculosis. After 6 mo of tuberculosis treatment (B panel), uptake was reduced.

Incidental thyroid lesions are often detected by PET/CT. Ono and colleagues from the Yotsuya Medical Cube (Tokyo, Japan) reported that in a review of the PET/CT records of 2,514 asymptomatic individuals, diffuse thyroid uptake was observed in 96 (3.8%). Localized thyroid uptake was seen in 26 (1%) individuals, and thyroid carcinoma was identified in 9 (38%) of these. Overall the PET-positive rate was 4.8%, and the positive predictive value in detecting thyroid lesions was as high as 95%.

Shie and colleagues from the Kaiser Permanente Fontana Medical Center (CA) and the University of North Texas Health Science Center (Fort Worth) reported on an even larger study of the prevalence of malignancy in incidental focal thyroid nodules identified by PET. (I want to pause here and parenthetically note how impressed I am with the number of studies at this meeting that included many results from patients across geographic and institutional boundaries. For many years we routinely heard presentations on 4 or 5 patients. Now, with an emphasis on evidence-based medicine and cooperative efforts, we are seeing studies with many thousands of patient records.) In this metadata review, published studies on 63,960 patients from 19 institutions were aggregated, and 672 of these patients had incidental focal thyroid ^{18}F-FDG uptake. Of these 672, 379 patients had associated records of histopathologic diagnosis, and 127 (33.51%) of these proved to

be malignant. The authors concluded that the high prevalence of thyroid malignancy associated with focal hypermetabolic thyroid nodules calls for needle biopsy when accumulations of ^{18}F-FDG are encountered incidentally.

Grassetto and colleagues from the Santa Maria della Misericordia Hospital (Rovigo, Italy) reported on the role of ^{18}F-FDG PET in the diagnostic work-up of patients with adrenal incidentaloma on conventional (MR/CT/ultrasound) imaging. The study included 74 patients with such findings, of whom 54 had histories of cancer. Significant ^{18}F-FDG uptake was found in 32 patients. At surgery, metastases were confirmed in all 28 of these 32 patients who had histories of cancer. The authors recommended PET as a "first-choice examination" to be performed in patients with oncologic histories and adrenal incidentalomas on conventional imaging.

Kiendys and colleagues from Ghent University Hospital (Belgium) reported on the prevalence and clinical significance of ^{18}F-FDG PET-positive incidentalomas. The retrospective review included the records of 5,476 whole-body PET/CT scans in patients, among whom 18 (0.3%) were found to have unexpected focal ^{18}F-FDG uptake in the parotid gland. Eight patients underwent surgery. Of these, 4 had benign tumors, 2 had infections, and 2 had metastatic disease. The authors concluded that ^{18}F-FDG PET-positive parotid incidentalomas are rare and focal uptake in this area can signal benign tumors, infection, or metastatic disease.

Yamane and colleagues from the Daiyuka General Hospital (Aichi, Japan) reported on the frequency of and clinical factors associated with incidental increased splenic uptake observed in ^{18}F-FDG PET. In a review of 5,577 patient records, increased splenic tracer uptake was observed in 209 individuals (3.7%). Uptake patterns were diffuse in 187 of these patients and nodular in 22. The group elucidated a range of causes for the unexpected uptake, the most common of which (131 patients, 63%) was related to the presence of previously unsuspected malignant lymphoma.

New Instrumentation and Radiopharmaceuticals

Many new instruments were introduced at this meeting. Among the trends seen is the advancing development of semiconductor imaging devices that provide good energy resolution and speed. Among their significant advantages is the elimination of phototubes, a feature that aids in fusing MR with either PET or SPECT in hybrid imaging. Nuclear imaging fusion with MR imaging, although the topic of at least a dozen papers at this meeting, is only in its beginning stages, and the use of these semiconductor instruments will be a tremendous boost in advancing new hybrid and single-modality innovations.

Figure 8 is a prototype brain PET scanner based on semiconductor detectors, described at this meeting by Morimoto and colleagues from Hitachi Ltd. (Ibaraki, Japan) and Hokkaido University (Japan). The scanner is based on the use of 18 cadmium telluride detectors, with a port diameter of 35 cm and an axial field of view of 25 cm without interplane septa. Initial performance evaluations reported by the developers indicate that the scanner is feasible for clinical use with high spatial resolution.

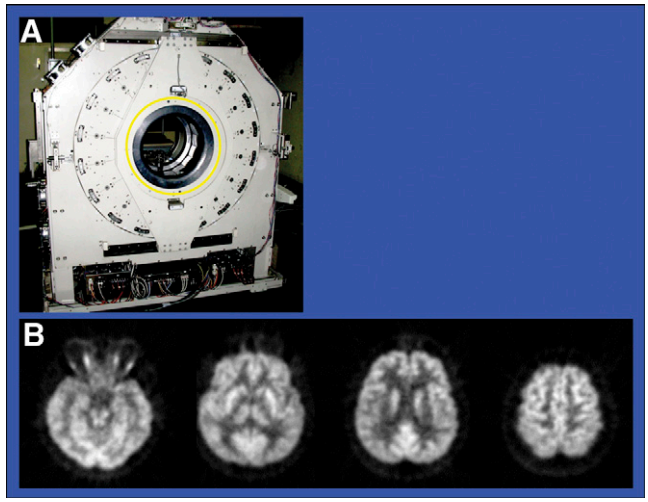

FIGURE 8. Prototype PET brain scanner (A) and example images (B) from Hitachi, Ltd., based on semiconductor detector technology.

From the same research group, Shiga and colleagues reported on the use of this device in identification of intratumoral inhomogeneous cell activity. Phantom and clinical tests suggested that the new PET device has the potential for better differentiation of differing cell activities within tumors because of higher resolution and less scatter noise. Figure 9 indicates that the new device provides better definition of lesions than either whole-body or brain scintillator PET and may provide advantages in treatment planning tailored to tumor inhomogeneity.

Lofton and colleagues from the University of Texas M.D. Anderson Cancer Center (Houston) reported on the performance characteristics of a portable pixilated cadmium telluride miniature γ camera (Fig. 10). The camera has a 32 × 32 element array, 44.8-mm^2 field of view, 1.2 × 1.2 × 5-mm element size, and an application-specific integrated circuit (128 elements × 8) with standard, high-resolution, and diverging collimators.

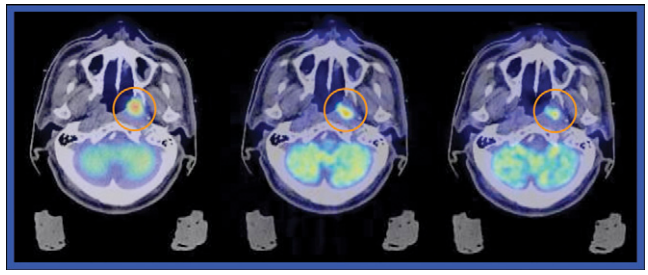

FIGURE 9. Image (right) acquired with the semiconductor device pictured in Figure 8 provides better definition of lesions than either whole-body (left) or brain (middle) scintillator PET imaging and may provide advantages in treatment planning tailored to tumor inhomogeneity.

FIGURE 10. Portable pixilated cadmium telluride miniature γ camera from AcroRad Co., Ltd.

O'Connor and colleagues from the Mayo Clinic (Rochester, MI) reported on molecular breast imaging as an adjunct to screening mammography. This is another important area in which molecular imaging techniques are used increasingly, with gains being driven by special-purpose devices. In this case, a cadmium zinc telluride γ camera (Fig. 11) provides excellent spatial resolution of 1.6 mm and energy resolution of ~4%. Figure 12 compares the conventional mammogram with breast molecular imaging, indicating that although a 20-mm lesion is seen on both modalities, an additional 10-mm lesion is seen only on breast molecular imaging.

Schilling and colleagues from Boca Raton Community Hospital (FL) reported on the utility of high-resolution positron-emission mammography in presurgical planning for breast cancer. Imaging results in Figure 13 suggest the various ways in which this approach is helpful in determining the extent of disease, in evaluating indeterminate lesions detected by MR imaging, and particularly in imaging patients with implants or dense breasts. In addition, excellent pathologic correlations are noted with the results of high-resolution positron-emission mammography.

Spanu and colleagues from the University of Sassari (Italy) reported on the value of preoperative planar scintimammography with a high-resolution dedicated breast camera (Fig. 14). The study included 44 patients (4 with bilateral disease, 24 with multifocal/multicentric invasive disease, and 16 with multifocal/multicentric in situ disease). Planar scintimammography was more accurate than mammography in 10 patients (22.7%), whereas conventional mammography was more accurate in only 1 patient (2.3%). The spatial resolution of this device is 1.6 mm, and the energy resolution is <5%. The images included in Figure 14 indicate that this allows visualization of much more detail in a multicentric invasive ductal carcinoma with an intraductal component, allowing the patient to be correctly staged and for operative management to be planned more precisely.

Piert and Guo from the University of Michigan (Ann Arbor) reported on a β/γ interoperative system designed to look for small pieces of remaining tumor after resection of breast cancer. The probes were developed because so many patients went to surgery soon (in some cases on the same afternoon) after ^{18}F-FDG studies. The new system was able to detect lesions even in the presence of high levels of residual background radiation.

FIGURE 11. Gains in molecular breast imaging are being made with apparatus like this cadmium zinc telluride γ camera.

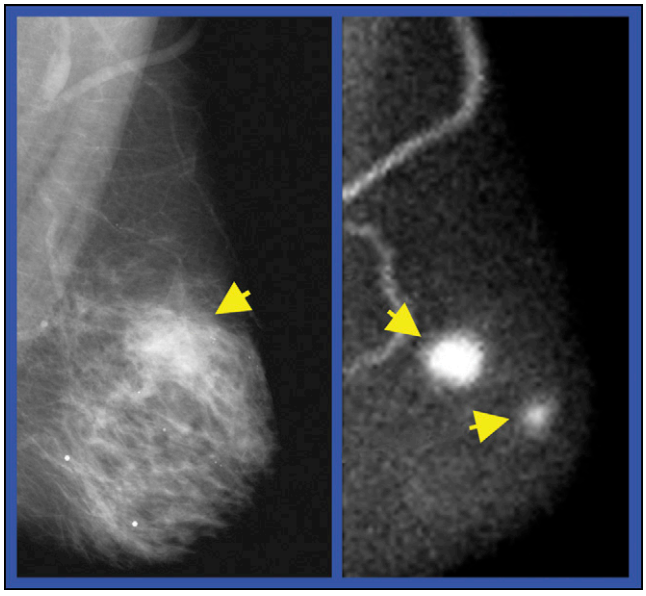

FIGURE 12. Although a 20-mm lesion is seen on both conventional (left) and molecular (right) breast imaging, an additional 10-mm lesion is seen only on molecular imaging.

Menard and colleagues from the Laboratoire IMNC (Orsay, France) and the Centre Hospitalier Universitaire Henri Mondor (Créteil, France) described a miniaturized intraoperative multimodal β-probe for brain tumor surgery. This probe is dedicated to real-time localization of residual tumor after the primary lesion has been excised. Direct coupling of the imaging device to the excision tool helps to simultaneously detect and remove residual tumor (Fig. 15). The ultrasonic aspirator fits inside the β-probe (Fig. 16). The small lesions peripheral to the resection site are localized and then immediately aspirated after ultrasonic destruction into particles.

In addition to new instruments, we need new radiotracers approved for a range of applications. In my opinion, the following radiotracers are currently ripe for approval and reimbursement: fluoride, fluorothymidine (FLT), hypoxia tracers, acetate, methionine, choline, fluoroethyltyrosine, and ^{18}F-DOPA.

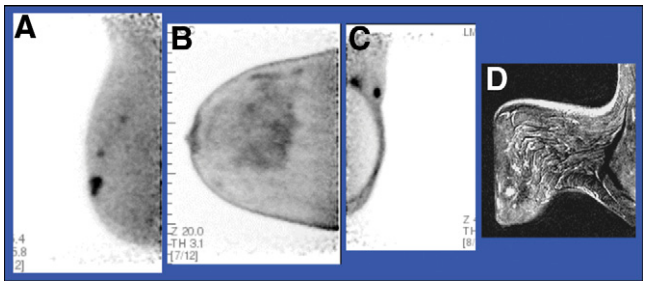

FIGURE 13. High-resolution positron-emission mammography is useful in presurgical planning for breast cancer by determining extent of disease (A), evaluating indeterminate lesions detected by MR imaging (B and D), and imaging patients with implants or dense breasts (C).

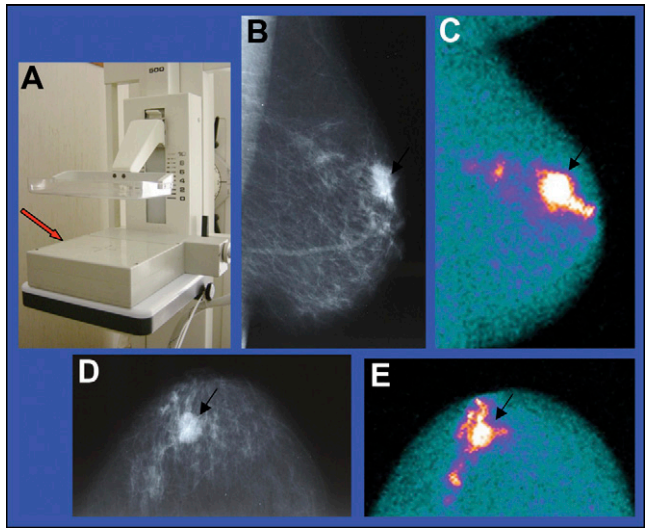

FIGURE 14. High-resolution dedicated breast camera from Gamma Medica-Ideas, Inc., used for preoperative planar scintimammography (A). Imaging allowed visualization of much more detail in a multicentric invasive ductal carcinoma with an intraductal component (C and E) than conventional imaging (B and D), allowing the patient to be correctly staged and for operative management to be planned more precisely.

Suleiman and colleagues from the U.S. FDA (Bethesda, MD) reported at this meeting that in 2007 75 Radioactive Drug Research Committees (RDRCs) submitted annual reports, summarizing 308 studies on more than 3,000 human research subjects. Two-thirds of the studies used PET nuclides. The researchers stated their belief that the FDA continues to believe that the RDRC program is an integral part of essential research for potential candidate drugs.

I want to offer a proposal for obtaining (and hastening) regulatory approval for this multitude of promising tracers. In this schema, physician- or industry-sponsored exploratory Investigational New Drug (eIND) applications are approved by the FDA for a small (e.g., 10 or 20) number of studies. The agent would then receive conditional approval, requiring cumulative evaluation for safety and effectiveness during further but indefinite clinical use. Each result from a patient study would be reported and included in a database that allows continual monitoring of safety and effectiveness.

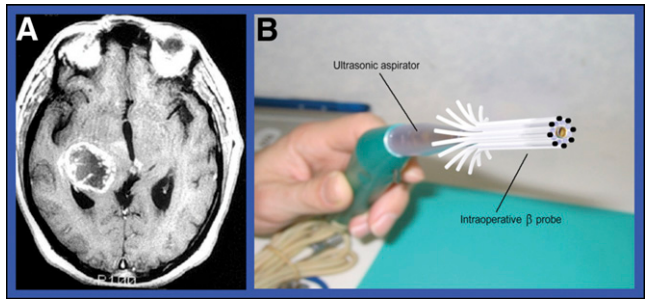

FIGURE 15. Miniaturized intraoperative multimodal β-probe for brain tumor surgery. Direct coupling of the imaging device to the excision tool helps to simultaneously detect and remove residual tumor.

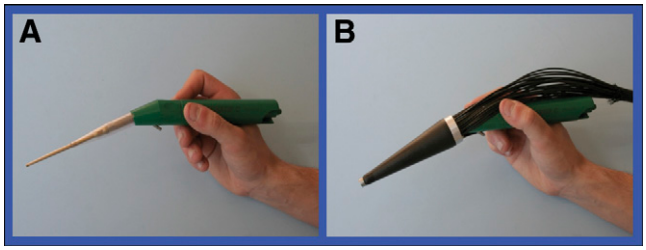

FIGURE 16. An ultrasonic aspirator (A) is coupled with the intraoperative β-probe (B) in the device seen in Figure 15.

This approach has recently been called "in-life testing" by Visiongain, Ltd. (London, UK), in the development of stable drugs. The result provides continuous, long-term (even perpetual) assessment of safety and effectiveness.

Another proposal for obtaining reimbursement for new molecular imaging biomarkers is to first determine the validity of the tracer for measuring a specific chemical process. Initial clinical studies would be performed after obtaining institutional RDRC or IND approval or an industry- or physician-sponsored FDA eIND. Hospitals or research grants would pay the costs of initial clinical research prior to approval for reimbursemet by CMS and others payors (I will explain later the economic model that might make them willing to do this). The medical and economic value of each study would then be assessed continually for all subsequent studies, with the results recorded in a national database.

A New Drug Application for radioactive tracers is a request for approval to market a new drug for a specific clinical use. The present requirement for approval is the legal requirement for "substantial" evidence of efficacy demonstrated through controlled clinical trials, which at the present time usually consist of hundreds and hundreds of patient studies assessing criteria such as outcomes, which may require long periods of time to yield definitive results. This requirement lies at the heart of the regulatory program for stable drugs but, in my opinion, should not be the basis of regulation of tracers. Tracers, unlike stable drugs, provide information analogous to that provided by measurements such as body temperature, blood pressure, or electrocardiographic data. Fewer patient studies should be needed before conditional approval.

CMS is the agency that determines whether a study will be reimbursed and should be made aware that the economic value of molecular imaging is a function of knowledge. I have discussed the following equation in previous Highlights Lectures: $dV/dt = f\mathrm{K}^*$, where V = value and K = knowledge. Correct decision making depends on knowledge, and this is different from clinical outcome. Increasing knowledge by molecular imaging is expensive, but making correct decisions decreases the cost of caring for each patient. The result may be an overall increase in institutional costs, because increasing productivity also increases demand for procedures, but ultimately the cost per patient decreases.

Local synthesis of tracers is a recurring focus at the SNM meetings. A few examples of ^{18}F-labeled tracers that could be synthesized within hospitals or regional facilities following the simplified regulatory process that I outlined here include: ^{18}F-DOPA for dopamine synthesis; ^{18}F-fluorouracil for pyrimidine analogs; ^{18}F-fluorotyrosine for large amino acid transport; ^{18}F-fluorocholine for membrane synthesis; ^{18}F-FLT for DNA synthesis; ^{18}F-fluorestradiol for estrogen receptors; and ^{18}F-fluoroazomycin arabinoside, ^{18}F-misonidazole, and ^{18}F-FRP-170 for hypoxia. The advantages of in-house production of radiotracers include easier regulatory approval, ever-increasing numbers of available tracers, ready availability, and decreased costs of care per patient. More than 40 y ago in *Nucleonics* I wrote that every hospital would have a cyclotron in 30 y. Although the timeline has slipped somewhat, I stand by the essential truth of that prediction.

Tabletop cyclotrons are being developed and commercialized. Ronald Nutt, PhD, with Siemens Medical Solutions (Malvern, PA), has a system with a beam energy of 7.5 MeV, which can produce 50 mCi of ^{11}C or ^{18}F. It cannot produce ^{13}N or ^{15}O. What they visualize and have already done in small numbers is "franchise" this biomarker generator for a $200,000 fee from the institution. Then the institution pays $100.00 per dose, with an agreement to produce a minimum of 8 doses per day. This approach of local production of PET tracers is, in my opinion, analogous historically to the conversion from mainframe to personal computers. I remember that in the early days, when computers were first introduced, the mainframe computers were behind a big glass screen, where it looked as if the computer experts inside were out of *The Wizard of Oz*. Today, although mainframe computers still exist, personal computers have become common, with the functionalities of the original mainframe now available to all PC users at their desks. Chemical synthesis in the tabletop cyclotron is based on microfluidics with glass-based liquid polytetrafluorethylenes. They are quite fast and have a high yield and low mass, which aids in making them nontoxic.

Another very important advance makes it possible to label almost any kind of peptide. McBride and colleagues from Immunomedics, Inc. (Morris Plains, NJ), and Garden State Cancer Center (Belleville, NJ) reported on a new method of ^{18}F labeling of peptides and proteins via a metal ligand. The rationale is that ^{18}F labeling usually attaches ^{18}F to carbon, a time-consuming and often multistep synthesis. Metal labeling of ligands is usually fast and can be carried out in a single step. The hypothesis of these investigators was that chelated ^{18}F-metal complexes may allow for rapid and efficient labeling of small molecules. They wanted to determine which metal(s) will form stable complexes with fluoride and be nontoxic at low doses. Fluorine binds to aluminum to form AlF_n complexes, which can perform several different functions in vivo. The peptide is labeled and purified in about 1 h, a method that can be

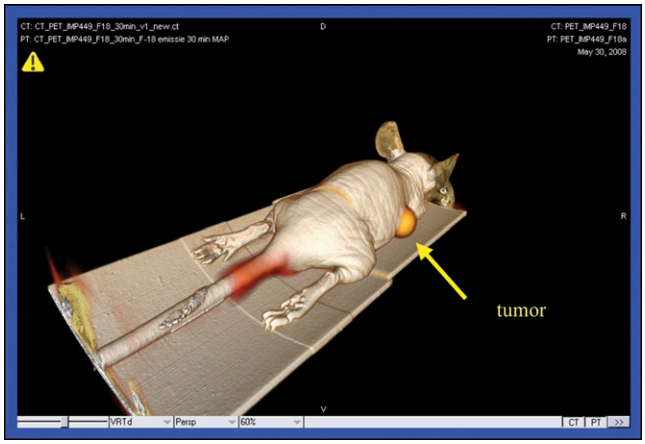

FIGURE 17. Al^{18}F-IMP peptide uptake in a colon tumor–bearing mouse pretargeted with anti-CEA anti-HSG bispecific antibody. Image shows uptake at 30 min in a 6-mm tumor.

applied to label almost any peptide ^{18}F. The group outlined initial work with combining a NOTA complex and Al^{18}F to label proteins and peptides in bispecific antibody pretargeting for immunoPET. Images from 3D mouse studies (Figs. 17 and 18) show the lesion quite clearly. The pretargeted Al^{18}F IMP 449 showed exceptional targeting in vivo, high tumor uptake, and excellent tumor-to-nontumor ratios within 1 h.

FIGURE 18. The in vivo peptide targeting technique shown in Figure 17 demonstrated high tumor uptake and excellent tumor-to-nontumor ratios, here seen in the same mouse at 1 h.

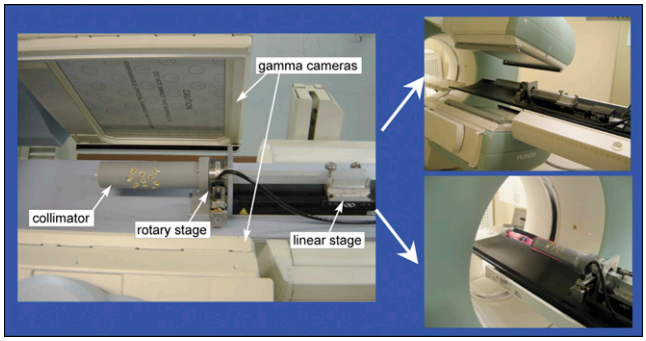

FIGURE 19. Multipinhole collimation device for small animal micro-SPECT/CT using a clinical scanner.

Small animal imaging devices have become widespread in academic chemistry and nuclear medicine departments. The growing availability of radiotracers made possible by in-house production is increasing interest in these studies, but not every department has access to a dedicated small animal scanner. Several groups at the meeting focused on devices for small animal imaging using clinical scanners. DiFilippo, from the Cleveland Clinic (OH), reported on a multipinhole collimation device for small animal micro-SPECT/CT using a clinical scanner (Fig. 19). Figure 20 shows some of the images obtained with this modified clinical instrument, including ^{99m}Tc-MAA lung micro-SPECT slices, coregistered CT, bone microSPECT, and micro-SPECT/CT.

Beekman and colleagues from University Medical Center Utrecht (The Netherlands) described very high-resolution SPECT with a dedicated high-resolution focused collimator based on pinholes. Figure 21 shows the USPECT-II with the 2 collimators, one for brain and one for whole body. Figure 22 provides an example of the quality of the images that can be obtained with .3 mm resolution compared with conventional CT imaging. Figure 23 is an example of ^{99m}Tc-HDP imaging with this device in a mouse.

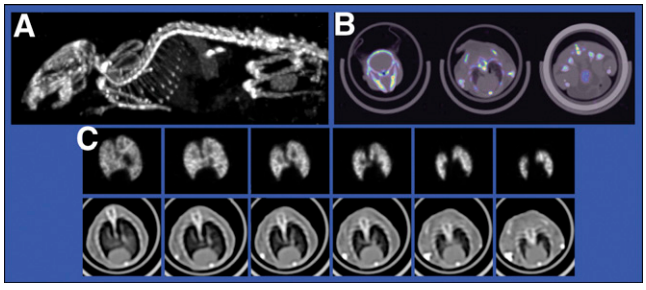

FIGURE 20. Images obtained with the device shown in Figure 19, including ^{99m}Tc-MAA lung micro-SPECT slices (C, top), coregistered CT (C, bottom), bone microSPECT (A), and micro-SPECT/CT (B).

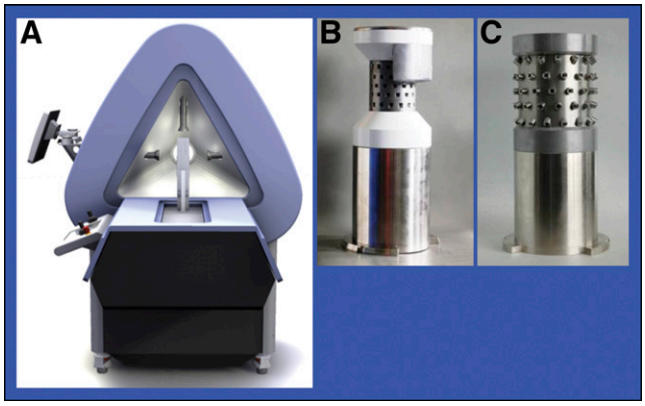

FIGURE 21. The USPECT-II (A) acquires small animal images with dedicated high-resolution focused pinhole collimators for brain (B) and whole body (C).

Cadmium telluride semidetector instruments are also being used in small animal PET scanners. Tanizaki and colleagues from Sumitomo Heavy Industries, Ltd. (Tokyo, Japan), and Tohoku University (Sendai, Japan) have developed a 512-channel detector device (Fig. 24) with bore size of 100 mm and transaxial and axial fields of view of 77 and 22 mm, respectively. Figure 25 shows images acquired with the device.

Kanai and colleagues from the Osaka University Graduate School of Medicine (Japan) and Tohoku University (Sendai, Japan) reported on rat brain studies acquired with ^{123}I-iomazenil and a semiconductor-based animal PET scanner. Figure 26 is a PET coronal section acquired with this in vivo technique and shows that the resolution is comparable with and superior to that of ex vivo autoradiography.

^{18}F-fluoride, in my opinion, should be first on the list for CMS approval because of its utility in imaging patients with bone metastases. Doot and colleagues from the University of Washington (Seattle) and the Seattle Cancer

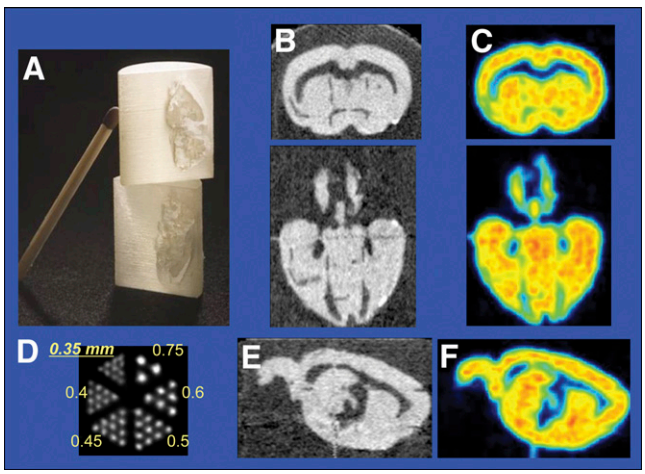

FIGURE 22. USPECT-II device 3D rat brain phantom (A) and resolution (D). Right panels compare CT (B and E) with U-SPECT images (C and F).

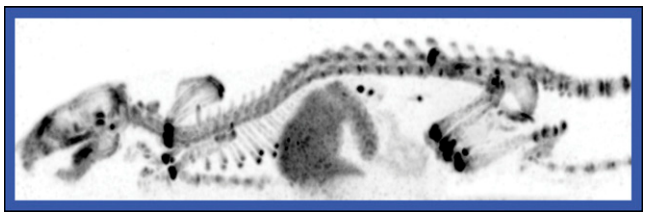

FIGURE 23. Example of ^{99m}Tc-HDP mouse imaging with the USPECT-II.

Care Alliance reported that kinetic analysis of ^{18}F-fluoride PET images can differentiate osteoblastic and osteolytic lesions in breast cancer metastases. The authors concluded that fluoride flux and transport can be accurately and independently measured for bone metastases and normal vertebrae (Fig. 27).

A negative ^{18}F-fluoride PET may occur in patients with malignant sclerotic bone lesions. Behesti and colleagues from the PET-CT Center and St. Vincent's Hospital (Linz, Austria) and King's College (London, UK) looked at possible reasons for ^{18}F-fluoride-negative PET in such lesions. In a study of 14 patients with known or suspected bone metastases, 31 malignant sclerotic lesions were identified with no ^{18}F-fluoride uptake. The mean density of these lesions was 1,221 ± 560 Hounsfield units, and they remained ^{18}F-fluoride negative despite disease progression and new metastatic formations in the other skeletal sites. In retrospective monitoring, 5 lesions were positive in previous ^{18}F-fluoride PET studies. The authors theorized that the lack of uptake could be the result of therapy response or apoptosis. Clearly ^{18}F fluoride is not perfect, but it remains a very good tool in our armamentarium.

Another example of a study with a large series of patients came from military experience at the Walter Reed Army Medical Center (Washington, DC). Kao and colleagues assessed the utility of skeletal scintigraphy for osteomyelitis evaluation in patients with amputations or

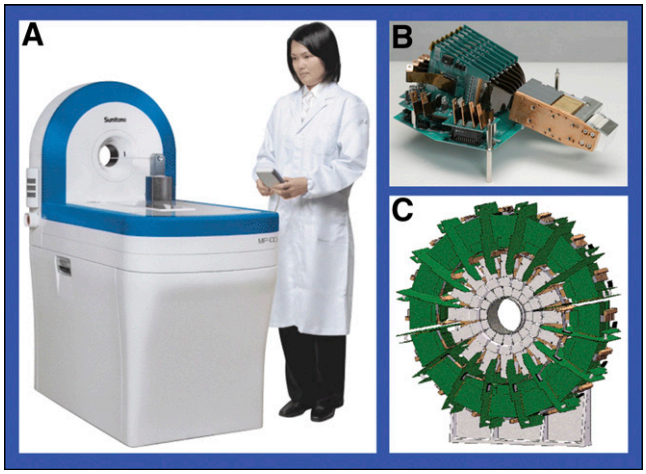

FIGURE 24. Ultra-high spatial resolution small animal PET scanner (A) using cadmium telluride semiconductor detectors (B and C).

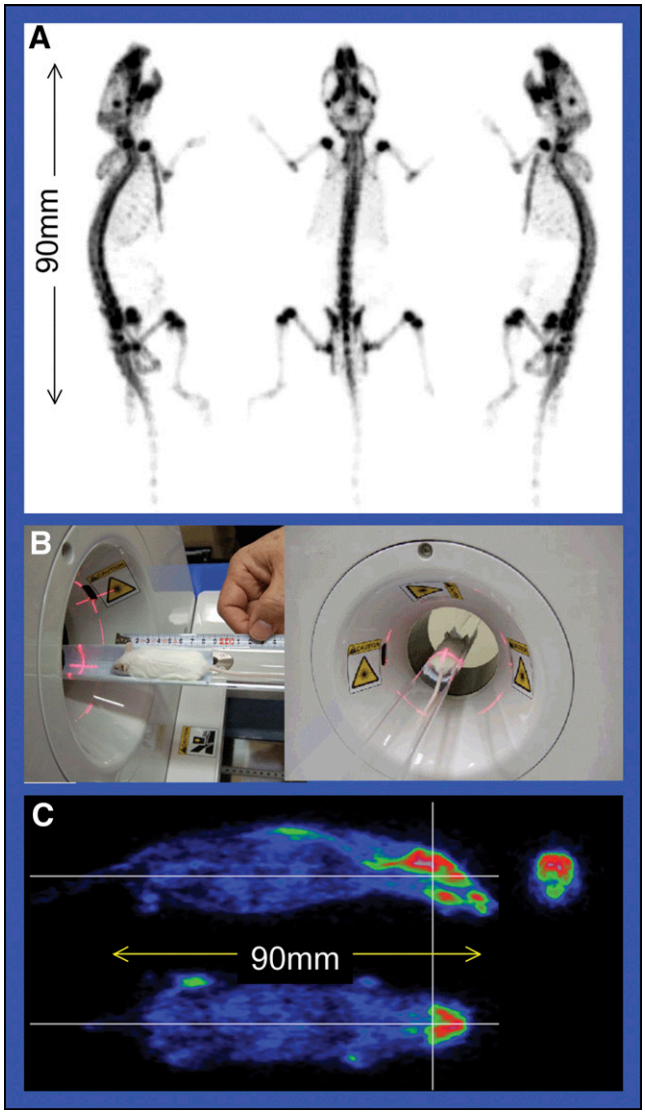

FIGURE 25. Images (A and C) acquired with the small animal PET scanner (B).

orthopedic devices. The investigators retrospectively reviewed all 3-phase bone scan reports for a 1-y period, with a total of 1,475 individuals. Inclusion criteria were an extremity amputation or current extremity orthopedic device and referral for potential osteomyelitis. Of the 29 patients who met these criteria, 28 (97%) scans had increased activity in the region of interest. Of these 28, 23 (82%) showed increased activity on all 3 phases of the examination. Twenty-seven were referred for ^{111}In-white blood cell/^{99m}Tc-sulfur colloid imaging to diagnose or exclude osteomyelitis. The investigators concluded that patients who have undergone an amputation or have an orthopedic device in an extremity should proceed directly to ^{111}In-tagged white blood cell/^{99m}Tc-sulfur colloid examination when osteomyelitis is suspected, stating that "skeletal scintigraphy provides little diagnostic benefit and results in unnecessary radiation exposure for this patient population."

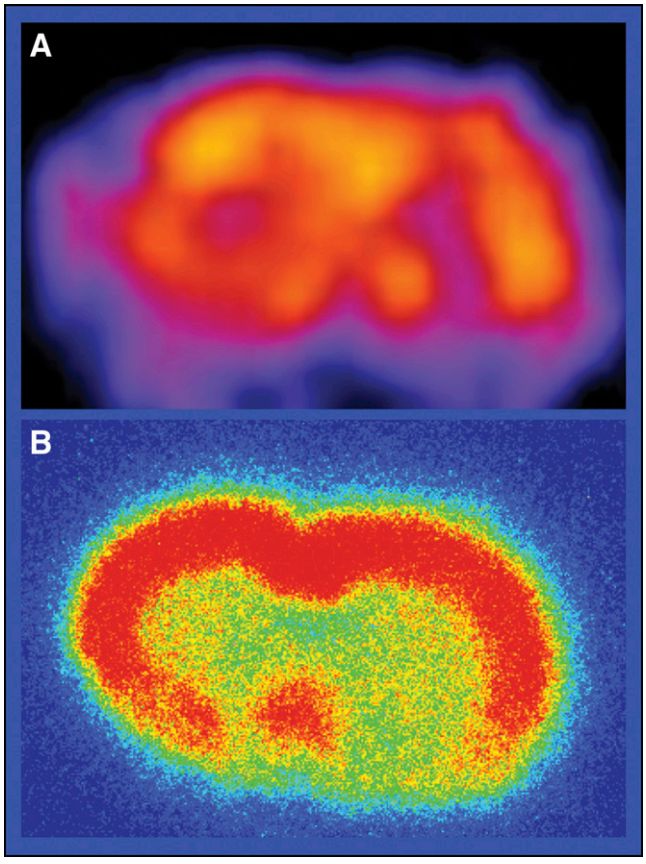

FIGURE 26. Coronal section image (A) acquired with ^{123}I-iomazenil and a semiconductor-based animal PET scanner is comparable with and superior to results from ex vivo autoradiography (B).

Herrmann and colleagues from the Technische Universität München (Germany) reported that ^{18}F-FLT helps in the characterization of proliferation and thereby in discriminating cancer from pancreatic pseudotumors. The study included 31 patients with undefined pancreatic

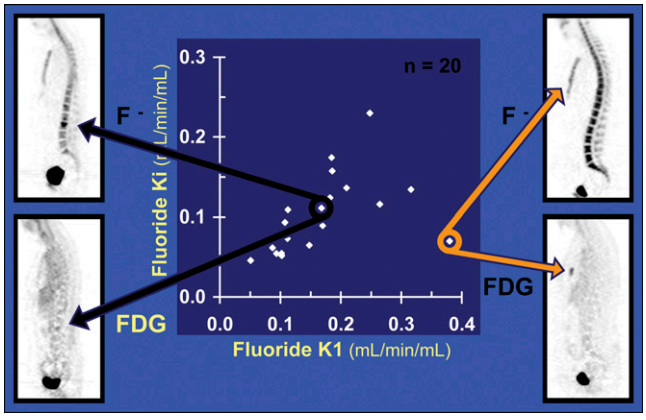

FIGURE 27. Kinetic analysis of ^{18}F-fluoride PET images can differentiate osteoblastic and osteolytic lesions in breast cancer metastases. The authors concluded that fluoride flux and transport can be accurately and independently measured for bone metastases and normal vertebrae.

tumors that were suspected to be malignant. All underwent ^{18}F-FLT PET, and focal uptake of the tracer was exclusively detected in malignant tumors; that is, a specificity of 100%. Fifteen of 21 malignant tumors, however, showed high focal uptake, for a sensitivity of 71%. It is important to remember that at any particular time, only about a tenth of the cells in even a very malignant tumor are dividing, so that although the signal with ^{18}F-FDG is 10 times that of ^{18}F-FLT, the accumulation of ^{18}F-FLT is more specific in showing cell division.

Souvatzoglou and colleagues from the same Technische Universität München group reported on the potential influence of ^{11}C-choline PET/CT on radiotherapy treatment planning in patients with biochemical recurrence of prostate cancer. ^{11}C-choline is now fairly widely used to study prostate cancer. In a study of 38 patients, these researchers found that the use of the labeled choline in an extended PET/CT radiotherapy plan was helpful in 5 patients (13%), contributing positively to individualized treatment planning and potentially improving the effectiveness of salvage radiotherapy. Figure 28 shows the conventional treatment planning and the incremental information provided by the addition of PET/CT data.

Nuclear Cardiology

Nuclear cardiology continues to advance. We are reminded with some frequency that the most common presenting manifestation of coronary artery disease (CAD) is still sudden death. Identification of those patients who are at significant risk remains extremely important. Piccini and colleagues from the Duke University Medical Center (Durham, NC) reported on SPECT myocardial perfusion imaging defects as strong predictors of sudden cardiac death in patients with CAD. Data they presented from a cohort of 6,383 patients with angiographically documented CAD who had also undergone gated SPECT imaging showed clear cut-off points in assessment of lesions and ejection fraction that predicted survival. When the summed stress score (SSS; i.e., blood flow as assessed by sestamibi studies) defects were <6 and the ejection fraction was >35, then survival rates were good. When the SSS was >6 and the ejection fraction was <35, then survival over the 12-y follow-up period was significantly lower.

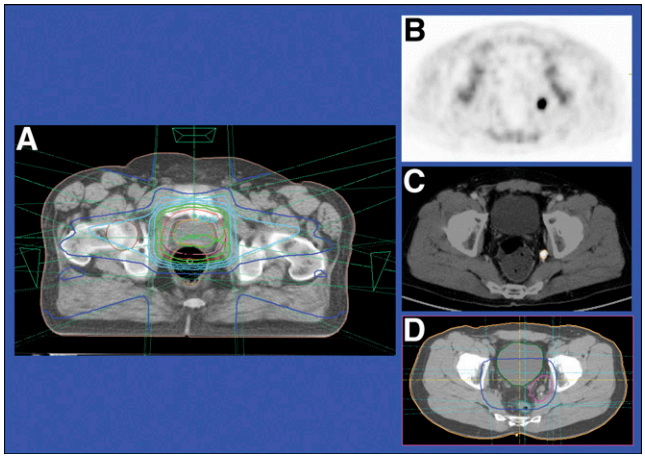

FIGURE 28. Conventional radiotherapy planning (A) was enhanced by data from PET (B) and CT (C) to provide a more precise PET/CT radiotherapy plan (D).

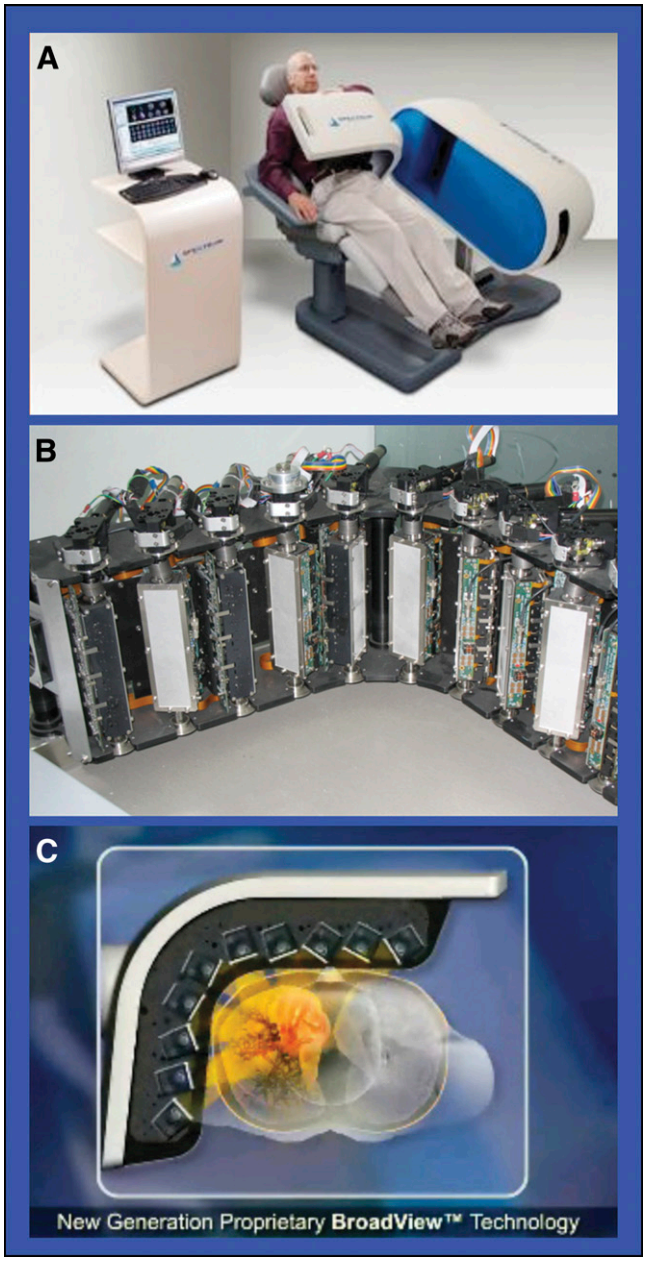

FIGURE 29. D-SPECT solid state cardiac SPECT scanner (A) and components (B and C).

Hutton and colleagues from University College (London, UK) and Spectrum Dynamics (Caesaria, Israel) reported on performance evaluation of the D-SPECT dedicated cardiac scanner (Fig. 29), which has a high sensitivity that facilitates high-quality dynamic studies. The improved energy resolution permits dual- or triple-radionuclide imaging, including the use of ^{99m}Tc, ^{123}I, and ^{201}Tl. The device permits the

acquisition of a stress study and rest study in a period of about 30 min rather than requiring separate rest and exercise examinations. Ben Haim and colleagues from the same research group reported on 11 patients in whom simultaneous dual-isotope myocardial perfusion imaging was acquired with the D-SPECT. The accuracy and image quality were equal to those of conventional myocardial perfusion imaging with separate stress and rest acquisitions.

CAD, as Javadi and colleagues from the Johns Hopkins University (Baltimore, MD) pointed out in a presentation at this meeting, is a continuum that can be characterized by PET, SPECT, and CT. The continuum begins with preclinical disease, which is accompanied by endothelial dysfunction and can be assessed by measuring coronary flow reserve. It then progresses to vascular remodeling and plaque formation, which can be measured by CT angiography, assessing the plaque burden. The progression is then to clinical disease, with flow-limiting stenosis or occlusion of the vessels. PET or SPECT can show regional ischemia or infarction. Our continued aim, of course, is to detect CAD as early along this continuum as possible.

I believe that the most important population that molecular imaging should be focusing on in this area is diabetic patients. A few example studies will explain why. Lautamäki and colleagues from the same Johns Hopkins University group that described the CAD continuum reported on quantification of myocardial blood flow with PET/CT and ^{82}Rb in a canine model of coronary artery stenosis. ^{82}Rb quantification of myocardial blood flow provides a new way to detect and assess CAD, making it possible to detect uniformly distributed (so-called "balanced") ischemia, which has been problematic. When all vessels are involved, initial distribution may appear normal, because we compare one region with another. These investigators showed that it is possible to more accurately monitor therapy as well as detect CAD with this approach that measures regional as well as balanced ischemia.

Yoshinaga and colleagues from the Hokkaido University Graduate School of Medicine (Japan) and the University of Ottawa Heart Institute (Ontario, Canada) compared ^{82}Rb with ^{15}O-water PET in the measurement of coronary endothelial function—the earliest changes that occur in the continuum of CAD. ^{82}Rb and ^{15}O-water myocardial blood flow estimates were well correlated over a wide blood flow range. Both identified altered flow response during cold pressor tests in smokers. The authors concluded that ^{82}Rb has a potential for wide clinical application, including the measurement of coronary endothelial function in smokers.

Lautamäki and the Johns Hopkins University group also looked at multitracer PET characterization of impaired myocardial sympathetic innervation in the viable infarct borderzone. Three different tracers were combined to investigate different components of presynaptic nerve biology. These included ^{11}C-epinephrine, which is normally stored in vesicles that protect it from metabolism; ^{11}C-hydroxyephedrine, which is avidly taken up but not metabolized; and ^{11}C-phenylephrine, which is not efficiently stored but leaks from vesicles and is degraded. Impaired neuronal biochemistry without complete denervation (the neurons are not completely damaged) contributes to arrhythmogenicity in the infarct borderzone, and this state may be reversible. The authors concluded that tissue heterogeneity and impaired innervation of viable myocardium are observed in the borderzone of myocardial infarct and show only partial agreement, so that these 2 arrhythmia markers are complementary rather than competitive and can be integrated into a single PET/CT session. Neuronal imaging can help develop novel antiarrhythmic therapies. Every year we see a few papers on sympathetic innervation of the heart, and I believe that these will continue to increase.

Kardan and colleagues from the Massachusetts General Hospital (Boston, MA) gave 2 presentations at this meeting on the characteristics of CardioPET, a modified fatty acid closely resembling naturally occurring fatty acids, as a cardiac PET tracer. As we know, the heart relies on fatty acids for most of its energy and, when stressed, begins to metabolize glucose. Figure 30 shows the CardioPET images in a healthy individual and a patient with CAD, which the authors noted were superior to myocardial perfusion SPECT in demonstrating coronary perfusion and detecting abnormalities in the myocardium in both rest and stress. Figure 31 is an example of the changing information that can be gathered from serial studies carried out from 3 min to 1 h after injection.

I believe that these and other techniques should be employed in looking for silent CAD in all patients with diabetes or risk factors as part of a concerted effort to

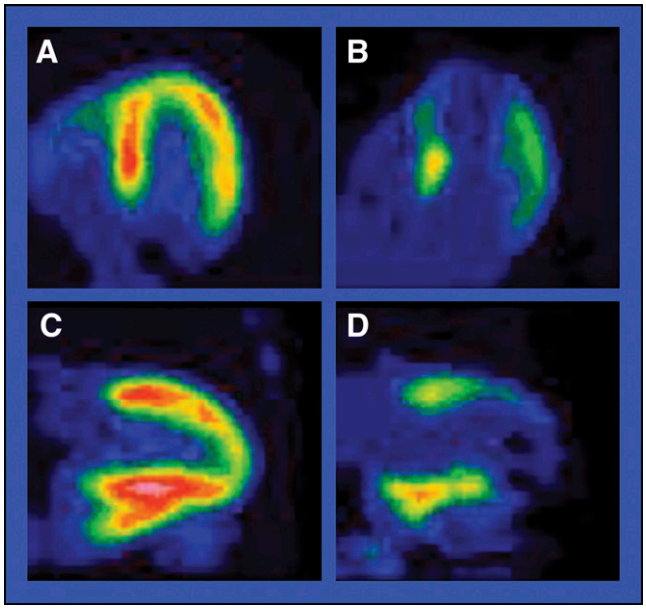

FIGURE 30. CardioPET, an ^{18}F-fatty acid analog, effectively demonstrated coronary perfusion and detected metabolic abnormalities in myocardium. Healthy volunteer (A and C); individual with coronary artery disease (B and D).

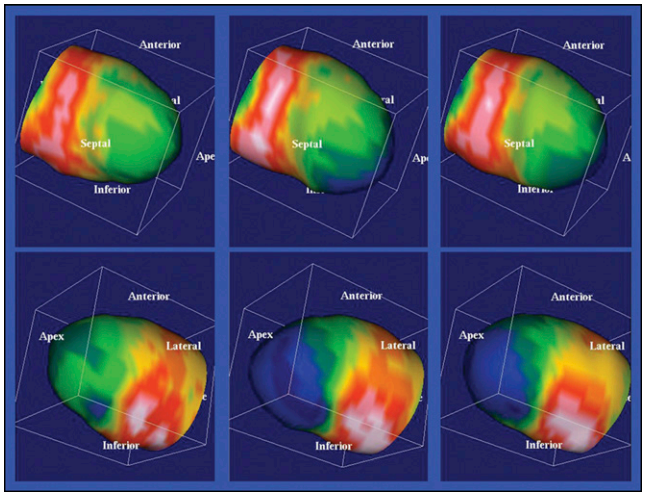

FIGURE 31. Example of changing information that can be gathered from serial studies carried out at 1–3 (left), 15–30 (middle), and 30–60 min (right) after injection of fatty acid analog tracer.

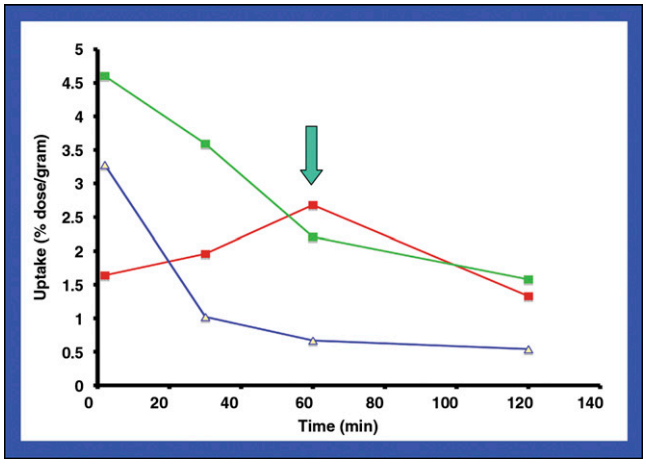

FIGURE 33. Distribution in rats of ^{18}F-epoxide FP-DTBZ, a tracer for vesicular monoamine transporter-2 and measurement of β-cell mass in the pancreas, indicates that the pancreas had the highest level of uptake of all organs or tissues.

encourage preventive measures. Why? We know that 34%−44% of patients with type 2 diabetes mellitus have coronary endothelial dysfunction, a functional precursor of CAD, without coronary artery calcification or abnormal increases in carotid intima-media thickness, as determined by ultrasound and electron beam tomography. Coronary endothelial dysfunction, which is the earliest sign of beginning CAD, can be detected by PET before structural alterations of the arterial wall can be seen.

Nkoulou and colleagues from the University Hospital of Geneva (Switzerland) reported on the results of ^{201}Tl SPECT screening of stressed-induced perfusion myocardial ischemia in a study population of 386 diabetic patients. Forty-four percent of symptomatic patients and 40% of asymptomatic patients were found to have perfusion defects (Fig. 32). This high percentage of "silent" myocardial ischemia led the authors to call for further studies to identify clinical predictors or algorithms that would select diabetic patients for myocardial perfusion screening.

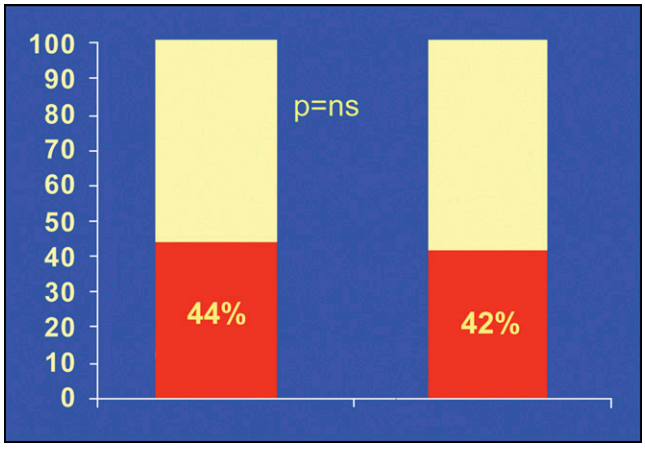

FIGURE 32. Percentage prevalence of perfusion abnormality in diabetic patients. Forty-four percent of symptomatic patients (left) and 42% of asymptomatic patients (right) were found to have perfusion defects.

Lieberman and colleagues from the University of Pennsylvania and Avid Radiopharmaceuticals, Inc. (Philadelphia), and the University of Michigan (Ann Arbor) reported on a new PET ligand for directly measuring β-cell mass in the pancreas, a capability of great importance in the diabetic patient. ^{18}F-epoxide FP-DTBZ is a tracer for vesicular monoamine transporter-2 (VMAT2) with high selective uptake. Figure 33 shows the tracer distribution in rats, indicating that the pancreas had the highest level of uptake of all organs or tissues. Figure 34 shows the localization of the tracer in the pancreas.

Ichise and colleagues from Columbia University (New York, NY) reported on another VMAT2 tracer, ^{11}C-DTBZ, for PET quantification of β-cell mass in the pancreas in diabetes. The study was conducted in patients with longstanding type 1 diabetes, a clinical situation in which β-cell mass may be almost depleted. Figure 35 shows accumulation of the tracer and binding in the pancreas, although the researchers noted that nonspecific binding may be a confounding factor in patients with longstanding diabetes.

Delbeke and colleagues from Vanderbilt Hospital (Nashville, TN) and Rambam Healthcare (Haifa, Israel)

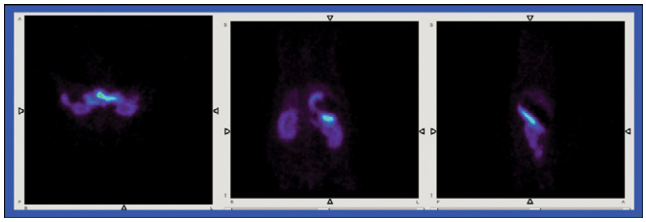

FIGURE 34. PET images of localization of tracer for vesicular monoamine transporter-2 and measurement of β-cell mass in the rat pancreas.

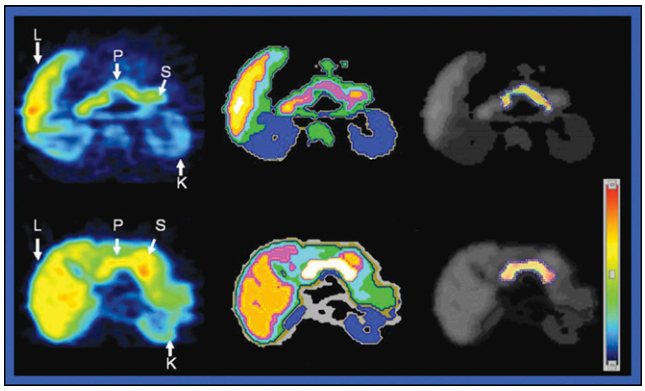

FIGURE 35. Images of ^{11}C-DTBZ accumulation in (top) patient with diabetes and (bottom) healthy volunteer. Left, summed tissue images; middle, tissue classification images; right, VMAT2 binding potential images.

reported on the effect of integrated rest/stress myocardial perfusion SPECT and 64-slice coronary CT angiography (CTA) on the management of symptomatic patients with an intermediate likelihood of CAD. They found that CTA was most helpful in decision making in 22% of patients with atypical CAD and 12% of patients with typical CAD. The 2 techniques were equally helpful in 47% of patients with atypical CAD and in 12% of patients with typical CAD. Both were important in 25% with atypical CAD and 75% with typical CAD. They concluded that the 2 imaging techniques are complementary and that the addition of a second noninvasive test avoided invasive procedures in more than 20% of patients.

Uebleis and colleagues from the University of Munich (Germany) reported on the value of calcium score and myocardial perfusion SPECT in the prediction of severe cardiac events during long-term follow-up in 260 patients with known CAD. Calcium score and myocardial perfusion scans were acquired within a 6-mo period. Over an average 5-y follow-up period (range, 0.2–10 y), calcium score and coronary stenosis were found to be strong and independent predictors of severe cardiac events. A total of 23 severe cardiac events (cardiac death or myocardial infarction) were recorded, and the highest annual event rate was in patients with calcium scores >400.

Inflammation is important in the pathogenesis and clinical outcome of atherosclerosis. Atherosclerotic plaque rupture results from inflammatory cell activity within the plaque. Plaques that contain numerous inflammatory cells (in particular, macrophages) have a high risk of rupture. Imaging techniques in current widespread use provide no indication of plaque inflammation. However, this is an area of research and investigation that is being explored with great success. By detecting regions of plaque instability through markers for inflammation, patients at risk can be treated to prevent future events. At Hopkins, for example, very few studies are performed in the nuclear medicine department on diabetic patients unless they come in via some other route or are referred for other reasons. I think that all of you in your own hospitals should begin to take a look at what molecular imaging can do for the diabetic population, remembering that approximately 40% of these patients will have CAD. Procedures that we are able to perform today and are exploring for tomorrow can have an effect on preventing the advance of disease by early identification and modification of risk factors.

Dresser and colleagues from the Harry S. Truman Memorial Veterans Administration Hospital and the University of Missouri (Columbia) reported on outcomes in patients with abnormal myocardial perfusion imaging and normal coronary angiography. In a retrospective review of 808 patients who had undergone both myocardial perfusion imaging and coronary angiography, 48 patients had abnormal perfusion imaging and normal coronaries seen in angiography. Sixteen of these patients were found to have had cardiovascular events over the follow-up period of 2–10 y, including 4 pericardial infarctions, 2 myocardial infarctions, 1 coronary artery bypass graft, 6 cerebrovascular events, and 3 peripheral revascularizations. The researchers concluded that myocardial perfusion imaging may predict a higher likelihood for cardiovascular disease than suggested by cardiac angiography alone.

Neuroimaging

I believe that clinical molecular imaging studies of the brain will eventually equal the number of studies in oncology or cardiology. Hwang and colleagues from the Seoul National University College of Medicine (South Korea) reported on gender differences in age-related decline in regional cerebral glucose metabolism. ^{18}F-FDG PET images were obtained in 230 healthy individuals (90 men, 140 women; age range, 34–82 y). Each sex was divided into 5 groups representing individuals in their 30s, 40s, 50s, 60s, and 70s and older. Imaging and quantitative results (Fig. 36) indicated that both men and women show significant age-related decline in cerebral glucose metabolism in similar regions of the brain. In men, however, the decline is fairly constant across the age group studies, whereas women go through patterns of steep declines in their 40s and 60s.

Shimosegawa and colleagues from the Osaka University Graduate School of Medicine (Saita, Japan) also studied gender differences in brain metabolism. The group reported on quantification of cerebral blood flow, cerebral blood volume, oxygen extraction fraction, and cerebral metabolic rate of oxygen with 3D high-resolution and high-sensitivity PET and ^{15}O. They found that women metabolize oxygen in the brain to a greater degree than men. Figure 37 shows images of cerebral oxygen metabolism and cerebral blood flow in women and men. The authors noted the need for separate normal absolute values for men and women.

Wang and colleagues from the Brookhaven National Laboratory (Upton, NY), St. Luke's–Roosevelt Hospital (New York, NY), and the National Institute on Alcohol Abuse and Alcoholism and the National Institute on Drug Abuse (Bethesda, MD) reported that binge eating is

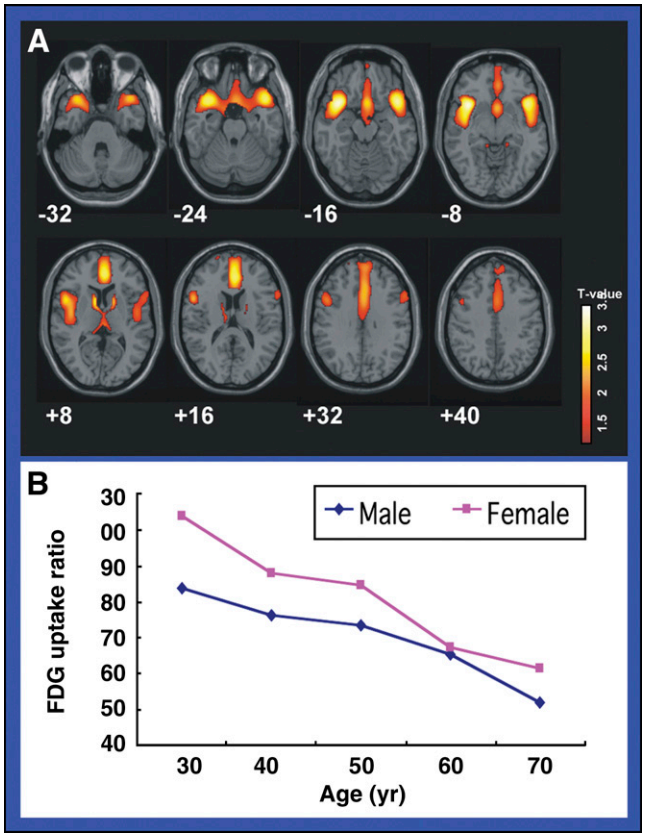

FIGURE 36. Men and women showed age-related declines in cerebral glucose metabolism in similar regions of the brain (A). In men, however, the decline is fairly constant across the age groups studied, whereas women go through patterns of steep declines in their 40s and 60s (B).

associated with dopamine increase during food stimulation. They showed a correlation between caudate dopamine release and the severity of binge eating disorder. Psychologists, with whom we work and should be working, have tests that can assess subjectively the degree of the eating disorder, and molecular imaging is providing quantitative support and validation of these tests.

The public has recently become much more aware of current diagnostic and treatment approaches to brain tumors through the well-publicized experience of Senator Ted Kennedy. It is important for us to make sure that the public also knows about the advantages that molecular imaging can bring in this disease setting. Wardak and colleagues from the David Geffen School of Medicine at the University of California at Los Angeles reported on the

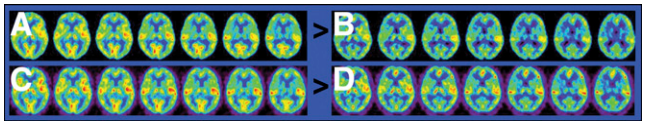

FIGURE 37. Gender differences in brain metabolism. ^{15}O PET indicates that women (A and C) metabolize oxygen in the brain to a greater degree than men (B and D). Top, cerebral oxygen metabolic rate; bottom, cerebral blood flow.

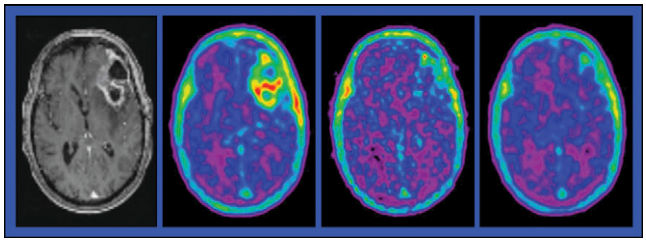

FIGURE 38. ^{18}F-FLT PET was useful in monitoring brain therapy. Left, baseline MR and PET. Right, evidence of changed uptake at 2 and 6 wk after initiation of bevacizumab and irinotecan therapy.

utility of ^{18}F-FLT PET in monitoring brain therapy. Figure 38 shows that within 2 and 6 wk after beginning therapy, tracer accumulation changed markedly in the tumor. When they looked at the change in standardized uptake values and performed kinetic modeling and discriminant analysis, this accumulation proved to be a good predictor of whether or not patients would survive for 1 y (Fig. 39).

Song and colleagues from the Sun Yat-sen University (Guangzhou, China) reported that ^{13}N-NH_3 PET is more sensitive and specific than Gd-DTPA MR imaging for diagnosing brain tumor. These authors compared imaging results from the 2 modalities in patients with 29 histologically confirmed brain tumors. For low-grade gliomas, ^{13}N-NH_3 PET had a 60% probability of lesion detection compared with only 20% for Gd-DTPA MR imaging. MR imaging was superior to PET in lesion detection of extra-axial tumors. Figure 40 shows imaging results in a patient with a grade 3 astrocytoma. The lesion demonstrated a markedly increased uptake of ^{13}N-NH_3 on PET but was only faintly enhanced in T1-weighted Gd-DTPA imaging.

In the 19th century, Broca (1861) and Wernicke (1874) related brain structure to function. Today, blood oxygen level–dependent (BOLD) functional MR imaging measures changes in regional brain blood flow and helps select regions of interest for molecular examination. With PET/CT and SPECT/CT, these approaches can provide a foundation for the molecular theory of brain disease, moving again beyond the cellular level to the molecular level. I

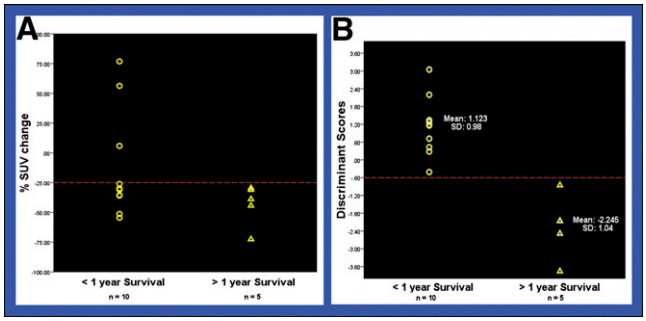

FIGURE 39. In the same study seen in Figure 38, percentage of standardized uptake value change at 6 wk after treatment (A) and scores from discriminant function (B) proved to be good predictors of whether or not patients would survive for 1 y.

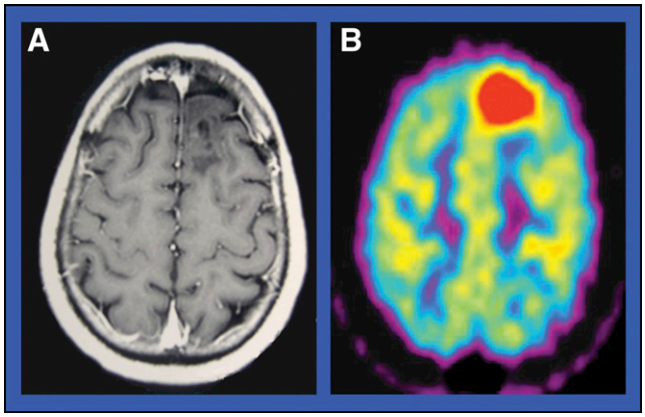

FIGURE 40. ^{13}N-NH_3 PET (B) had a 60% probability of lesion detection compared with only 20% for Gd-DTPA MR imaging (A). This example is in a patient with a grade 3 astrocytoma.

should note that this is the 25th anniversary of the first imaging of a neuroreceptor in the human brain. Dopamine receptors were first imaged on May 25, 1983.

A number of tracers are currently used for molecular imaging in the brain. These include but are not limited to: ^{18}F-FDG, $^{13}NH_3$, and ^{15}O; dopamine receptor agonists and antagonists; serotonin receptor agonists and antagonists; adrenergic receptor agonists and antagonists; monamine transporters (NE, DA, 5-HT); adenosine receptors and transporters; vesicular transporters (VMAT2, VAChT), cholinergic receptor agonists and antagonists; GABA/benzodiazapine receptors; opiate (μ, κ, Δ, and σ) receptors; peripheral benzodiazapine receptors; excitatory amino acids (glutamate) receptors; NMDA and AMPA receptors; neurotensin receptors; and histamine H_3 receptors.

eINDs are a novel regulatory mechanism used to provide proof of action, evaluate pharmacokinetics, select the most promising agent from a group of lead candidates, and determine their biodistribution. eINDs require less preclinical support than traditional INDs. The toxicology requirements are simpler, as are the dosimetry, pharmacokinetics, and metabolism required in animal models, with low tracer dose and low radiation exposure. eIND applications to the FDA have been used in the evaluation of ^{18}F-labeled PET amyloid plaque imaging agents, as reported in a multiinstitutional study by Pontecorvo and colleagues from Avid Radiopharmaceuticals (Philadelphia, PA), Duke University (Durham, NC), University of Michigan (Ann Arbor), Mayo Clinic (Rochester, MD), Washington University (St. Louis, MO), and Johns Hopkins University (Baltimore, MD). They compared 4 novel imaging agents. Figure 41 shows the striking accumulation of ^{18}F-AV-45, an amyloid imaging agent now in phase 2 clinical development.

Villemagne and colleagues from Austin Hospital, the National Ageing Research Institute, and the University of Melbourne (Melbourne, Australia) reported on a longitudinal study of β-amyloid deposition using ^{11}C-PiB PET to predict conversion to mild cognitive impairment (MCI) or

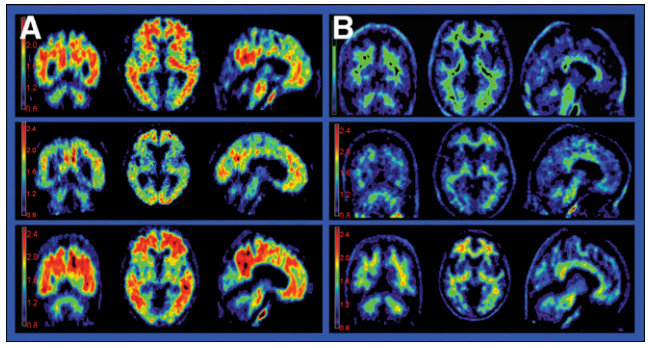

FIGURE 41. ^{18}F-AV-45 is an amyloid imaging agent in phase II clinical development. PET imaging in individuals with Alzheimer's disease (A) and in healthy controls (B).

Alzheimer's disease (AD). The study included 35 healthy controls and 28 individuals with MCI or AD who were observed over a 21-mo period. Among the 25 healthy controls who were PiB-negative on PET, only 1 (4%) converted to MCI over the follow-up period. Of the 10 healthy controls who were PiB-positive, 3 (30%) converted to MCI or AD. In the group with MCI or early AD, 13 individuals were PiB-negative, and 5 (385) converted to dementia. The 15 remaining individuals in this group were PiB-positive, and 12 (89%) converted to AD over the follow-up period. The overall changes in the amyloid-β burden over 21 mo were small (6.4% in AD). However, as is clear from this and other studies, the amyloid-β deposition occurs well before the onset of AD. PiB-positive healthy controls are at increased risk for cognitive decline, and most PiB-positive MCI patients convert to AD within 2 y. PiB-negative patients with MCI may be more prone to develop non-AD dementia, such as multiple infarct dementia. PiB PET is an excellent predictor of conversion to AD.

Yeung and colleagues from the Hong Kong Sanatorium and Hospital and the University of Hong Kong (China) reported on a practical method for 3D imaging of cerebral localization of ^{11}C-PiB PET in an investigation of AD and compared the information provided by this technique with that from ^{18}F-FDG PET. Figure 42 shows avid accumulation of the PiB compound in amyoid plaques using the authors' subtraction technique.

Deeb and colleagues from the University of Pittsburgh Medical Center (PA) compared the merits of visual

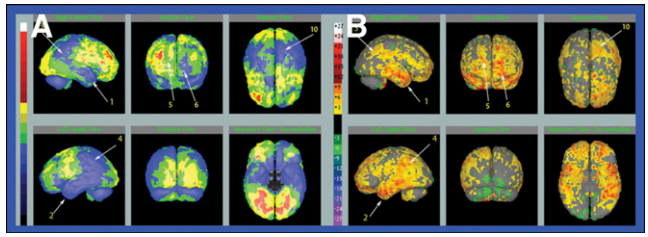

FIGURE 42. 3D ^{11}C-PiB PET imaging (B) shows avid accumulation of tracer in amyloid plaques, contrasted with ^{18}F-FDG PET imaging (A).

diagnosis and statistical software analysis of ^{18}F-FDG PET images to distinguish between normal, MCI, and AD individuals. The study included 19 elderly normal controls, 17 individuals with MCI, and 16 individuals with AD. They found that in general visual assessment provides a fairly accurate ability to distinguish between controls and AD, but that this accuracy significantly increases with the statistical software.

Forster and colleagues from the Ludwig-Maximilians University (Munich, Germany) reported on ^{18}F-FDG PET and cortical representation of visual/spatial abilities in patients with AD. We are all familiar with the increasingly popular drawing tests to screen for AD, a process that is roughly analogous to stress testing in nuclear medicine. In this study, performance on a simpler standardized drawing exercise (Fig. 43A) was correlated with ^{18}F-FDG uptake in the right hemispheric visual association cortex, which belongs to the dorsal visual stream and is involved in the processing of localization information. Performance in an analytically more complex task (Fig. 43B) correlated with uptake in structures of the ventral visual stream, which are involved in high-level visual processing and object recognition. These regions of the brain become abnormal early in dementia.

Kendziorra and colleagues from the University of Leipzig (Germany) and the University of Zurich (Switzerland) reported on 2FA-PET imaging in elaborating differences in cerebral nicotinic acetylcholine receptors in patients with stable MCI and in MCI patients converting to AD. In patients who converted to AD, tracer accumulation was markedly diminished in the cingulate cortex, hippocampus, and the temporal cortex. The authors point to this technique as a potential tool in predicting conversion from MCI to AD.

Hattori and colleagues from the University of Washington, Seattle Pacific University, Minor and James Medical Center, Veterans Affairs Puget Sound Health Care System, and Seattle Nuclear Medicine (all of Seattle) reported on cognitive fatigue after mild traumatic brain injury as an indication of frontocerebellar functional dissociation. The study included 15 patients who were imaged with ^{99m}Tc-ECD SPECT at rest and after activation with the Paced Auditory Serial Addition Test (another psychological stress test). Persons with a history of mild traumatic brain injury had less neuronal activation and fewer neurons than the control subjects when attempting to carry out a task. Figure 44 compares results from a normal control and a patient with mild traumatic brain injury.

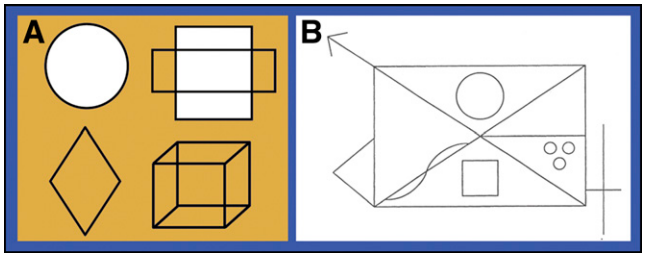

FIGURE 43. CERAD drawing test (A) and Rey Osterreith Complex Figure drawing test (B) for dementia assessment.

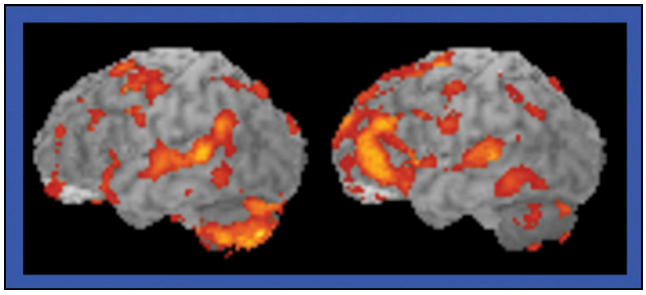

FIGURE 44. ^{99m}Tc-ECD SPECT in a person with a history of mild traumatic brain injury (right) showed less neuronal activation and fewer neurons than in a control subject (left).

Prunier-Aesch and colleagues from the CHRU Bretonneau and the University François Rabelais (Tours, France) reported on the use of ^{123}I-IBZM SPECT dopamine receptor imaging in patients with parkinsonian syndrome. This technique has already found success in differentiating between Parkinson's disease and so-called Parkinson-plus syndromes (multiple system atrophy and progressive supranuclear palsy). This group studied 99 patients with ^{123}I-IBZM SPECT, automated partial volume correction techniques, and a 2-y follow-up. They found that imaging was able to differentiate between Parkinson's disease and Parkinson-plus syndromes and that the partial volume techniques increased specificity.

Brašić and colleagues from the Johns Hopkins School of Medicine (Baltimore, MD) reported on the correlation of dopamine release and psychiatric symptoms in individuals with Tourette's syndrome. The study group included 18 adults with and 10 healthy adults without Tourette's syndrome. Psychiatric rating scale assessments were performed throughout 2 consecutive PET scans during which each individual received high-specific-activity ^{11}C-raclopride after saline and amphetamine challenges.

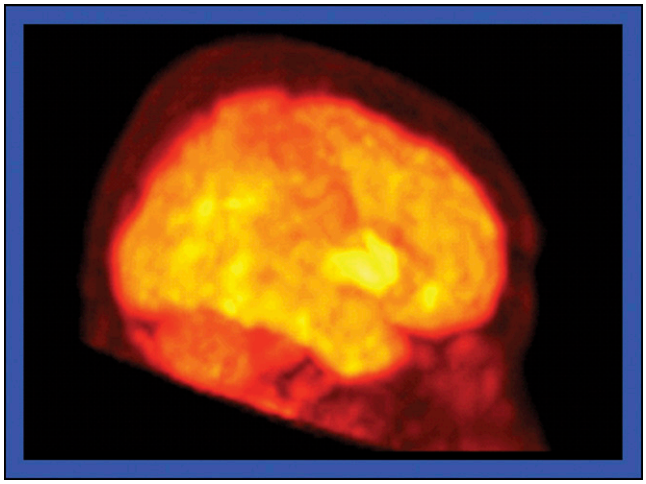

FIGURE 45. 3D view of ^{11}C-GSK 215083 distribution in the human brain, with high uptake in striatal regions.

The researchers found that in adults with Tourette's, the release of dopamine in striatal regions correlates strongly with behavioral changes.

New types of neuroreceptors are being imaged. Martarello and colleagues from the GSK Clinical Imaging Center and Imperal College (London, UK) reported on the first human evaluation of ^{11}C-GSK 215083, a high-affinity 5-HT$_6$ serotonin receptor antagonist with potential useful applications in AD. 5-HT$_6$ serotonin receptors are the latest receptors to be identified by isolating defined DNA sequences and then obtaining multiple copies. Figure 45 is a 3D view of tracer distribution, with high uptake in striatal regions.

Volkow and colleagues from the Brookhaven National Laboratory (Upton, NY) and the National Institute on Drug Abuse (Bethesda, MD) provided evidence that modafinil at therapeutic doses blocks the dopamine transporter in the striatum by 50% and reduces ^{11}C-raclopride binding to dopamine receptors by 6%. Modafinil is prescribed to treat narcolepsy, tiredness, and sleep apnea and is under investigation as a treatment for drug addiction. It is frequently used off-label by persons in jobs demanding wakefulness (military pilots on long missions) and as a cognitive enhancer (*Nature.* Professor's little helper. 2008;450:1157). The authors found in this study that levels of dopamine transporter blockade after therapeutic doses of modafinil are equivalent to those after therapeutic doses of methylphenidate (ritalin), suggesting that synaptic dopamine-enhancing mechanisms are relevant in the therapeutic effects of modafinil. Because drugs that elevate brain dopamine have the potential for abuse, these findings raise concerns about the possible abuse of modafinil.

One question that is now being asked and that molecular imaging is in a position to explore is: should we try to improve mental function in normal people? Volkow and colleagues also looked at the mechanisms by which methylphenidate enhances attention. Using ^{18}F-FDG PET they studied 21 healthy adults tested at baseline and while performing a numerical task with and without methylphenidate pretreatment (Fig. 46). They discovered that with methylphenidate the brain required ~50% less glucose to perform tasks equally well. One of the mechanisms of methylphenidate, then, is to improve the efficiency of the human brain.

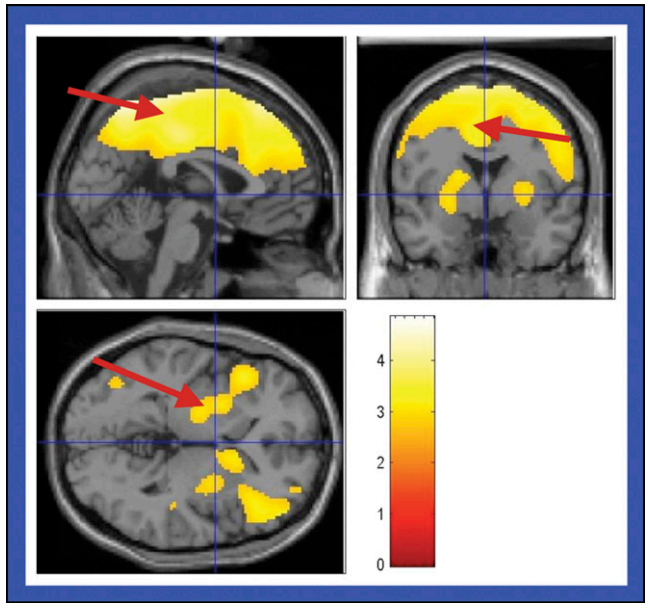

FIGURE 46. ^{18}F-FDG PET showed increased regional glucose metabolism in the parietal cortex, singulate cortex, and striatum when individuals performed numerical tasks with methylphenidate pretreatment.

Final Thoughts

Molecular imaging is now part of the big business of health care. In 2006, only 13 new drugs were approved by FDA, although $27 billion were spent on research and development. Pfizer and Johnson and Johnson, for example, spent well more than $7 billion each. Worldwide sales of prescribed drugs totaled more than $600 billion per year. Laura Wood wrote on the Web resource Research and Markets that, "The challenges facing large pharmaceutical companies are stark: sales are slowing, and research and development costs are rising. There is an overwhelming need to reduce development costs by as much as 30%−40%, while at the same time significantly shortening development cycle times."

Molecular imaging is in an increasingly advantageous position to help develop new drugs at lower cost and to decrease the complexity and invasiveness of many procedures. One example can be seen in the work of Moulin-Romsee and colleagues from the CHU St. Louis and the Institut Curie (Paris, France), who reported that in the PET era routine bone biopsy is no longer necessary in staging patients for Hodgkin's disease. The study included 14 patients with newly diagnosed Hodgkin's leukemia who had undergone both ^{18}F-FDG PET/CT imaging and a bone marrow biopsy. PET/CT was found to be more sensitive than biopsy in the detection of lesions as a result of the sampling limitations of biopsy. The authors concluded that bone marrow biopsy is not justified in patients with pretreatment negative PET/CT.

It takes more than good science to move research from the laboratory into medical practice. It is clear from this year's SNM meeting that many people are very actively involved in the molecular imaging movement. Molecular imaging is at a "tipping point." We need to educate the public, press, and our political leaders about the revolutionary effect that molecular imaging can have in creating a medical theory of disease and health care.